

POLITECNICO DI TORINO

Master's Degree in Electronic for Industrial
Application



**Politecnico
di Torino**

Master's Degree Thesis

Peltier Module Powered Embedded System

Supervisors

Prof. Massimo VIOLANTE

Ing. Alessandro BERGAMINI

Ing. Antonio PIRRO

Candidate

Gabriele TROVATO

11/04/24

Summary

The thesis in question, developed in collaboration with a toll company, aims to create a prototype device for the aforementioned company that is innovative and environmentally friendly. The goal is to utilize heat transfer to make the embedded system even more long-lasting and durable, achieved through an energy harvesting process based on Peltier cells. Firstly, the Peltier cell is analyzed in detail, examining its physical-chemical composition and revisiting classical literature topics such as P-N and P-N-P junctions. The optimal use of these tools is demonstrated, along with mathematical formulas to calculate the heat sink that aggregates on one of the cell faces. Secondly, a synthesis of lithium batteries is presented, primarily focusing on their main characteristics and methods to understand their State of Charge (SoC). This is crucial for determining the type of battery needed to create a circuit capable of recharging the Peltier cell. Furthermore, the topic of energy harvesting is explored, including its definition, categorization, and various types. This is a highly innovative area, particularly valued by modern companies increasingly investing in innovation. Chapter 6 details the analysis, characterization, and experimentation of the device. The mechanism used to characterize the Peltier cell is described, along with the data obtained and related considerations. The response of the Peltier cell to the driver enabling energy harvesting operation is demonstrated, supported by graphs and tables to aid understanding. Additionally, the chapter covers the characterization of the lithium battery used by the company, including estimations of its charge capacity duration and heat resistance. Finally, the circuit designed to enable communication between the three elements - Peltier cell, battery, and energy harvesting module - is presented. The mechanical design of the device is also showcased since it is an embedded system to be placed inside the vehicle cabin, attached to the windshield. This requires a specific mechanical setup to allow the antennas in the toll system to function in parallel with the Peltier cells, which are attached to the windshield to collect heat and operate effectively.

Acknowledgements

ACKNOWLEDGMENTS

*“A chi Ha il Coraggio di
Andare avanti nonostante Tutto”*

Alla fine anche noi siamo arrivati ad ottenere questo traguardo importante. Parlo al plurale perchè l'obbiettivo raggiunto è di carattere personale, ma se sono riuscito a tagliare il traguardo il merito è anche vostro. Solo voi, chi più chi meno, com'è gusto che sia, siete a conoscenza delle rinunce fatte per poter essere qui oggi; Solo voi siete a conoscenza della fatica fatta e del sacrificio dedicato a questa causa. E' sempre grazie a voi e al vostro supporto se sono arrivato alla stesura di questo progetto di tesi e alla fine dei miei studi, (per questa parte di vita).

Chi mi conosce lo sa, non sono una persona facile da gestire o da capire, però voi siete riusciti nell'impresa di sopportarmi per tanti anni e vi meritate queste parole: Innanzitutto, un grande ringraziamento al mio relatore Ing. Massimo Violante, sempre pronto a guidarmi in ogni fase della realizzazione della tesi. Grazie a lui ho accresciuto le mie conoscenze e le mie competenze.

Non posso esimermi dal ringraziare l'azienda presso la quale ho svolto il mio tirocinio formativo, Telepass, per avermi dato questa importante opportunità. Ritengo una grande fortuna aver avuto la possibilità di svolgere il mio lavoro di tesi in un ambiente lavorativo così interessante e dinamico, che mi ha permesso di mettermi in gioco e fare un'esperienza che sarà preziosa per il mio futuro. Da questa opportunità ho conosciuto persone eccezionali come i miei colleghi Ing. A. Bergamini, Ing. P. Cassini, Ing. D. Colamarino, Ing. F. Fasano, Ing. D. Gonella, che ringrazio e che sono diventati una seconda famiglia e con i quali spero di avere tante altre esperienze da condividere.

Ringrazio l'azienda TXT-ETech nella persona del Ing. A. Pirro e Dott.ssa M.Zuardi

per avermi dato la possibilità e la fiducia di iniziare questa esperienza.

Ringrazio la mia famiglia che in questi anni ha gioito con me per ogni esame superato ma anche sofferto per quelli non andati bene; abbiamo sofferto per la distanza che in questi anni ci ha tenuti separati, ma nonostante ciò il legame è rimasto intatto, se non più forte, con la consapevolezza di esserci sempre gli uni per gli altri nelle occasioni importanti.

In particolare ringrazio mia Madre che mi ha sempre lasciato libero di prendere la mia strada, anche se questa porta lontano dal nido materno, mi ha dato la libertà di poter sbagliare ed assumermi le conseguenze che ne derivano e questo mi ha fatto diventare la persona che sono oggi. La mia stima nei suoi confronti e in quella della mia famiglia anche se non lo lascio a vedere è immensa, perchè è gente che nonostante le intemperie della vita non si è mai lasciata abbattere, è andata avanti fino ad ottenere le proprie soddisfazioni.

Ringrazio mia sorella Giuliana, persona squisita che nelle mie giornate "No" bastava una sua chiamata per tirarmi su di morale, ti auguro di andare avanti sulla strada e raggiungere i tuoi obiettivi.

Ringrazio tutti i miei nonni, anche chi durante il percorso ci ha lasciato, perchè se abbiamo una bella famiglia il merito è soprattutto il loro.

Ringrazio tutti i miei zii con i quali nonostante le distanze e i vari impegni abbiamo avuto sempre modo di sentirci e confrontarci. Su tutti i miei parenti di Genova che nei primi anni mi hanno dato una mano importante.

Ringrazio i miei cugini che mi hanno sempre dimostrato il loro supporto e affetto, in particolare Lorena venendo spesso a trovarmi. Ringrazio i miei amici, pilastri importanti di questa mia esperienza qui a Torino. Amicizie nate tra i banchi universitari, consolidate tra una bevuta e l'altra e diventate amicizia vera nel corso degli anni. Con loro ho fatto di tutto, dai progetti universitari fatti fino alle 3 del mattino, fino alle discussioni sul senso della vita. Dalle gite fuori porta alle feste in casa. Voi siete stati parte FONDAMENTALE di questo percorso, compagni di vita e quando arriverà il giorno di separarci lo faremo con la consapevolezza di essere importanti gli uni per gli altri e con la consapevolezza di aver vissuto davvero anni indimenticabili. Vi ringrazio TUTTI.

Ringrazio anche le persone che oggi non fanno più parte della mia vita e quelle che non hanno creduto in me, anche loro sono stati importanti nella mia crescita personale.

Alla fine un ringraziamento lo devo fare anche a me. Ti ringrazio Gabriele perchè hai la testardaggine di non mollare mai e di raggiungere sempre i tuoi obiettivi, non perdere mai questa caratteristica.

Table of Contents

List of Tables	VIII
List of Figures	IX
1 Introduction	1
1.1 Basic Principle	2
1.2 The physical structure	3
1.2.1 Seebeck Effect	3
1.2.2 Peltier Effect	4
2 The semiconductor theory applied to Peltier cells	7
2.1 The semiconductor cell	7
2.1.1 Semiconductor theory	7
2.2 PN junction and semiconductor junction	8
3 Peltier Cell	11
3.1 The structure of the semiconductor Peltier cell	11
3.2 Thermoelectric modules (TEC)	14
3.3 Electrical connections	16
3.4 Application	17
3.5 Technical parameters	18
3.5.1 The thermal gradient	19
3.6 Dissipating the heat from the hot side	19
3.7 Benefits of thermoelectric generators	20
3.8 Static cooling systems	22
3.8.1 Dissipator Calculate	23
3.8.2 The practical use of cells	24
3.8.3 Damage due to condensation	26
4 Energy Harvesting	27

5	Lithium Battery	30
5.1	Chemical Composition	30
5.1.1	Lithium-ion Battery	30
5.1.2	Disadvantages of Lithium Cells	31
5.1.3	Advantages of Lithium Cells	32
5.2	Functions of a BMS	32
5.2.1	BMS Architectures	34
5.3	SoC & SoH	34
5.3.1	State of Charge SoC	34
5.3.2	Estimation of SoC: Methods	35
5.3.3	State of Health (SoH)	41
6	Analysis and Results of the Thesis Project	43
6.1	Battery characterization	43
6.1.1	Constant current discharge	43
6.1.2	The discharge with a constant resistance	45
6.1.3	Consideration	45
6.2	Battery Temperature Test	48
6.2.1	Result	50
6.3	Characterization Peltier Cell	50
6.3.1	Example calculation of Peltier cells using simplified formulas	51
6.3.2	LT-Spice characterization	53
6.3.3	The device structure with a Peltier cell	58
6.3.4	Cell & Harvesting	60
6.3.5	Case	62
A	Reference	67

List of Tables

1.1	Seebeck Coefficient	4
4.1	Summary Application	29
5.1	Differences Between Battery Types	31
6.1	Summary Application	44

List of Figures

1.1	Peltier Cell	2
1.2	Peltier Effect	5
1.3	α Characteristic	6
2.1	P-N Junction	10
3.1	P-N Junction on Peltier Cell	12
3.2	P-N Junction - When current enters the P-type region on the left and exits from the right, the junctions at the top cool down while those at the bottom heat up.	13
3.3	P-N Junction - When current enters the P-type region on the right and exits from the left, the junctions at the top heat up while those at the bottom cool down.	14
3.4	15
3.5	TEC Structure	16
3.6	Heant Sink	21
3.7	Termic Resistence	22
3.8	23
3.9	Cross-sectional area	25
5.1	Basical Principle	31
5.2	BMS Chart	33
5.3	BMS Architectures	35
5.4	Open Circuit Voltage	37
5.5	Model Base	39
5.6	Kalman Filter	40
5.7	Neural Network	40
6.1	Hardware	44
6.2	Discharge Curve	45
6.3	Discharge Curve General Market	46
6.4	Discharge Curve	47

6.5	Comparison	47
6.6	Test Curve	48
6.7	Block Diagram	49
6.8	Switch Block Diagram	50
6.9	T peltier / T environment	51
6.10	T peltier / Res Heatsink	52
6.11	T peltier / CPU Watts	52
6.12	LT-Spice config	54
6.13	Harvesting Scheme	59
6.14	Harvesting Curve	60
6.15	Test 1	61
6.16	Test 2	61
6.17	Test 3	62
6.18	Exploded View	63
6.19	Transversions Section	63
6.20	Scan View	64
6.21	Case	64

Chapter 1

Introduction

The thesis focuses on the development of an innovative and environmentally friendly prototype device in collaboration with a toll company. The device aims to utilize heat transfer for prolonged durability through an energy harvesting process using Peltier cells. The thesis delves into the detailed analysis of Peltier cells, including their physical-chemical composition and classical literature topics such as P-N and P-N-P junctions. Mathematical formulas for calculating heat sink are provided. A synthesis of lithium batteries is presented, emphasizing their characteristics and methods for understanding their State of Charge (SoC) to determine the appropriate battery for recharging the Peltier cell. The exploration of energy harvesting includes its definition, categorization, and various types, reflecting its significance in modern companies' innovation efforts. Chapter 6 focuses on the analysis, characterization, and experimentation of the device. It describes the mechanism used to characterize the Peltier cell, presents data, and demonstrates the cell's response to the energy harvesting operation. The chapter also covers the characterization of the lithium battery, estimating its charge capacity duration and heat resistance. The thesis concludes by presenting the mechanical design of the device is highlighted, considering its placement inside the vehicle cabin attached to the windshield. This specific setup accommodates antennas in the toll system to function in parallel with the Peltier cells, ensuring effective heat collection and operation.

In this chapter, we will get to know the Peltier cell that is the protagonist of our project. We will examine its chemical-physical characteristics, the operating principle of the device, and its most common applications.

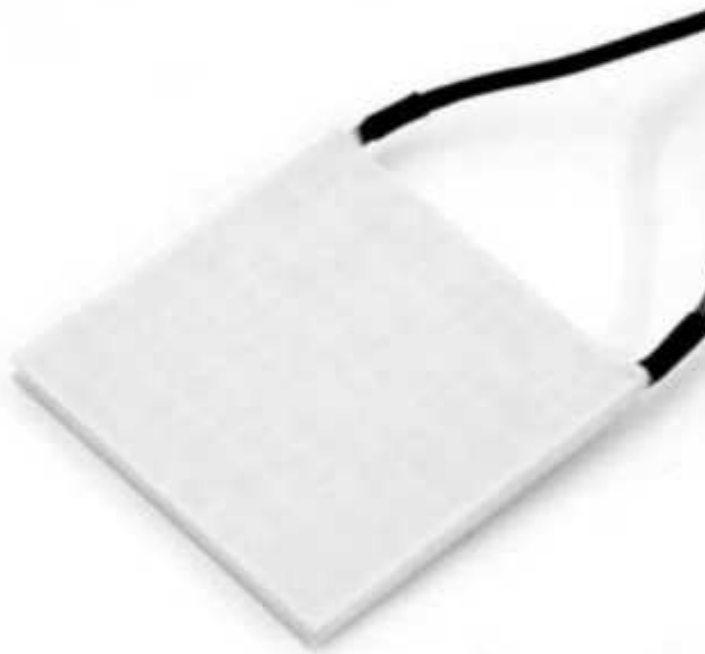


Figure 1.1: Peltier Cell

1.1 Basic Principle

The Peltier cell is an electronic component capable of generating a temperature difference between its two surfaces when crossed by an electric current: by supplying power to its two terminals, the cell heats one of its faces (which is thus called the hot side) and cools the other (which is thus named the cold side). Externally, it appears as a wafer composed of two square or rectangular plates, which enclose a lattice of square columns; both plates are made of alumina, a synthetic ceramic material with high thermal conductivity, except that while the cold side is made of natural alumina, the other (hot side) is usually coated with a layer of copper. This is because copper is an excellent heat conductor and can dissipate heat. The cell consists of the junction, which is the union of two different metals welded together; the structure is designed to expose the junction, which rests on a sheet of thermally conductive material. In practice, multiple junctions are joined together, electrically connected in series, and structured so that all those of one type are supported by a conductive sheet and those of the other are contact with a second sheet: the Peltier cell in the physical sense is the junction of two different metals (or even differently doped semiconductors, as will be explained later). In practice, when referring to a Peltier cell today, the latter is meant, also known as a Peltier cell thermoelectric module or TEC (Thermo Electric Cooler).

1.2 The physical structure

An elementary Peltier cell is nothing more than a double junction between two metals; from Physics, we know that by joining two metallic elements of different nature, the difference in their atomic structure determines, at the ends of the resulting junction, a very small potential difference.

1.2.1 Seebeck Effect

The elementary junction formed by the union of two metals exhibits another characteristic: when heated, the potential difference across its ends increases, but not only that: the polarity changes depending on which of the two sides is heated. "This occurs due to what is called the Seebeck effect, who discovered it in 1821".

¹ Thanks to this thermoelectric effect, a junction between two different metals behaves like a voltage generator: precisely, a thermoelectric pile, characterized by having practically zero internal resistance, thus being able to deliver certainly limited voltages but currents of high intensity. The same principle enunciated by Seebeck is the basis of the operation of thermocouples, precise temperature sensors that can even be immersed in molten steel and respond with a voltage to the heat they are exposed to.

The potential difference V obtainable from a Peltier cell used as a thermoelectric generator is expressed by the simplified formula:

$$V = (S_a - S_b) * (T_2 - T_1) \tag{1.1}$$

Where S_b and S_a are the Seebeck coefficients of the two metals, and T_2 and T_1 are the temperatures of the two junctions. The formula holds assuming constant (although they actually vary slightly with temperature) Seebeck coefficients within the temperature range considered by the application. "The Seebeck coefficient can be either negative or positive, depending on the type of metal", like show in table by Wikipedia.²

¹Introduction to Vibration Energy Harvesting

²Seebeck coefficient, Wikipedia

Material	Seebeck coefficient relative to platinum ($\mu * V/K$)
Selenium	900
Tellurium	500
Silicon	440
Germanium	330
Antimony	47
Nichrome	25
Iron	19
Molybdenum	10
Tungsten	7.5
Gold, Silver	6.5
Copper	6.5
Rhodium	6.5
Lead	4
Aluminium	3.5
Carbon	3
Mercury	0.6
Platinum	0
Sodium	-2
Potassium	-9
Nickel	-15
Bismuth	-72

Table 1.1: Seebeck Coefficient

1.2.2 Peltier Effect

The junction between two metals produces voltage and current, thus effectively functioning as an electrical generator. Even when creating two junctions, with one metal inside and another outside (Figure 1.2), heating one of the two creates an imbalance, as the potential increases in one compared to the other.

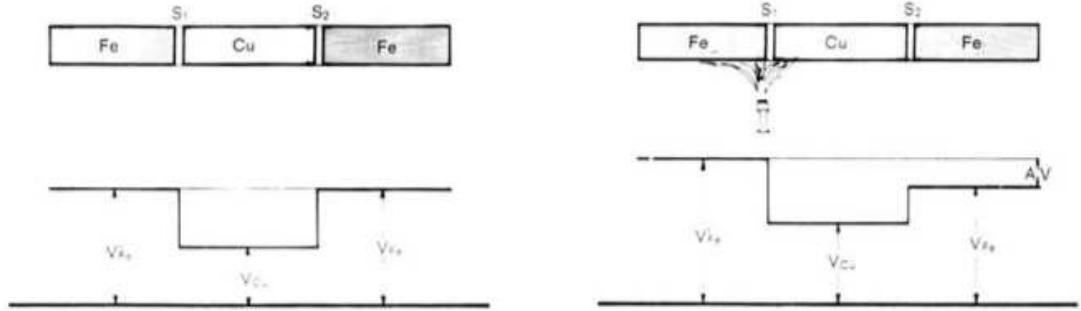


Figure 1.2: Peltier Effect

The Seebeck effect manifested in such a system is reversible; by passing current through the structure, an interesting phenomenon occurs: depending on the direction, one side heats up while the other cools down. The temperature difference between the two sides is more pronounced with higher current passing through the junction. The phenomenon described here is known as the Peltier effect, named after Jean Charles Peltier who discovered it back in 1834. His experiment involved a set of three pieces of metal welded together in a row, two of them being identical and one of a different metal (such as platinum and rhodium or antimony and bismuth), forming two junctions. Depending on the current passing through them, the metallic portions reached a more or less significant temperature difference. Moreover, Peltier also discovered that by reversing the direction of the current, the situation reverses as well, meaning that the previously warm parts become cold and the cold part becomes warm.

$$Q_p = \pi * I = a * T * I_a = \text{SeebeckEffect} \quad (1.2)$$

"where I is the electrical current flowing in the thermoelectric module, π is the Peltier coefficient that can be expressed by means of Seebeck coefficient α ".³

³Modeling and Simulation of Thermoelectric Energy Harvesting Processes

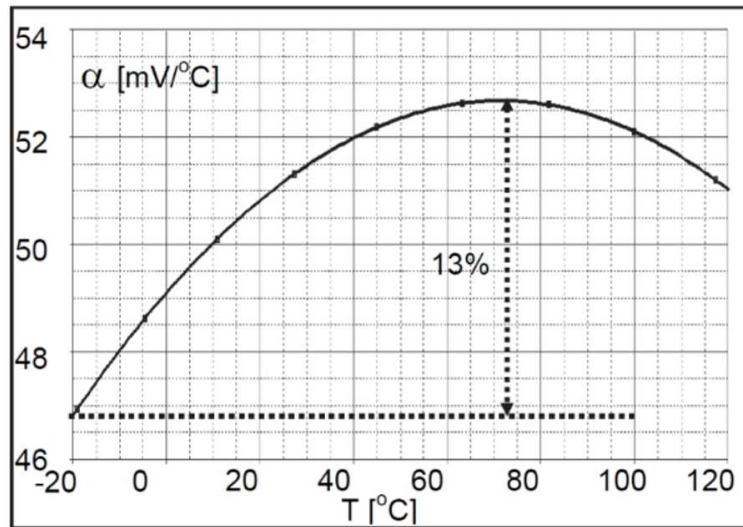


Figure 1.3: α Characteristic

The discovery, certainly interesting and full of prospects, was never practically exploited because metal junctions have too much thermal conductivity and do not allow, as they still do not allow, substantial temperature differences between the hot and cold sides to be achieved. It happens, therefore, that the heat produced on the hot side tends to pass very easily to the cold side, bringing the two temperatures closer together and reducing the thermal gradient.

Chapter 2

The semiconductor theory applied to Peltier cells

In this chapter, a comprehensive overview of semiconductors is provided, with a detailed analysis of the doping phase. This chapter is foundational as it allows us to understand in detail the junction, a key element of the Peltier cell.

2.1 The semiconductor cell

An elementary cell, that is, a single element of the lattice that typically constitutes what is commonly referred to as a Peltier cell, is composed of a PN junction, albeit realized with a particular architecture that allows for the exposure of the junction zones. Semiconductor technology has perfected processes capable of easily and inexpensively working with silicon and, generally, semiconductor materials; for this reason, it has been and still is convenient to manufacture Peltier cells using semiconductors.

2.1.1 Semiconductor theory

To increase the conductivity of semiconductors, elements are introduced into the crystal lattice that enrich the structure with available electric charges for conducting any current; this introduction is called doping, and the element introduced into the semiconductor is called a dopant. When the introduced impurities are trivalent, the doping is referred to as P-type, while the introduction of pentavalent elements determines N-type doping; in the former case, there is an electron deficiency, while in the latter, there is an excess. This occurs because silicon and germanium atoms have a valence of 4, so by introducing trivalent atoms into the semiconductor, the structure created has fewer electrons (one less for each dopant atom), while adding

pentavalent atoms results in an excess of electrons (one for each atom doping the semiconductor).

Examples of N-type dopants (pentavalent) are arsenic, antimony, and phosphorus, while among the P-type dopants (trivalent) are aluminum, boron, and gallium; those with a valence of 5 are called donors (because they donate electrons to the semiconductor structure, which is tetravalent), while the trivalent ones are called acceptors (because they have an electron deficiency and thus predispose the tetravalent structure to accept them). The doping operation is carried out in various ways, depending on the technique used to produce semiconductor components:

- In the case where the semiconductor is created by growth on radiofrequency crystal or in a linear radiofrequency furnace, once the semiconductor ingot is obtained, it is inserted into a second high-temperature furnace where the diffusion process takes place: the semiconductor is heated and dopant elements are introduced into the furnace from one side, reaching the surface and penetrating the crystal lattice due to the intense heat.
- On the other hand, if epitaxial growth is utilized, the semiconductor grows on a reference layer onto which gaseous molecules are deposited (for example, in the case of silicon growth, trichlorosilane), which precipitate from the top of the furnace after reacting chemically and releasing semiconductor atoms. In this case, doping occurs by adding impurities to the gas molecules.
- Finally, for specific synthetic semiconductors such as gallium arsenide, epitaxial growth exclusively occurs by introducing gases containing both arsenic and gallium, in varying quantities depending on the type and desired doping level for the semiconductor to be synthesized.

2.2 PN junction and semiconductor junction

The semiconductor Peltier cell is based on a pair of junctions between differently doped semiconductor materials, meaning it is a structure formed by three pieces of semiconductor welded together: two N-types at the ends and one P-type in the middle, or vice versa. In other words, it could be considered the combination of two junctions of differently doped semiconductors: PN and NP. However, it should be clarified that the semiconductor cell is not a PN junction, nor is it an NPN structure like that, for example, which forms the bipolar transistor. To understand this, let's briefly see what a PN junction is and how it works, which is the basis of many semiconductor electronic components: The PN junction is a bar of semiconductor doped on one side with pentavalent impurities and on the other with trivalent elements; the region doped with atoms with a valence of 5 is called the N region (or cathode) and is rich in electrons outside the crystal lattice, while the region with

trivalent doping (anode) is rich in holes (vacancies) left by the deficiency of valence electrons. At the boundary between the P and N regions, the excess electrons in the pentavalent part, which have not inserted into the tetravalent structure of the semiconductor, move to fill the holes left by the trivalent atoms in the P part. This creates a third region, called the depletion zone because there are no free electric charges in it; this prevents the conduction of current. To make the PN junction conduct, a potential difference of opposite value to that (potential barrier) created across the depletion region must be applied to the ends of the depletion region. The voltage must be positive on the anode (P region) with respect to the cathode (N region) to push the excess electrons in the N region towards the P region; its value must exceed the threshold value, corresponding to the electric potential needed to remove the electrons that have filled the holes near the depletion region from the holes themselves. By reverse biasing the junction, i.e., with the anode (P region) negative with respect to the cathode (N region), the effect of reinforcing the potential barrier is obtained: the component does not conduct, except for the very weak reverse saturation current, until, when the breakdown voltage is exceeded, the junction breaks down and conducts. The semiconductor Peltier cell, on the other hand, is a soldering joint between two semiconductor pieces doped in the same way and one doped in the opposite way, so two of N-type and the other of P-type or vice versa. The single junction of P and N elements, compared to the PN junction, differs both structurally and functionally, as follows:

- The junction is not a single block of semiconductor doped on one side with P and on the other with N, but it is the physical union of two parts;
- The surface of the junction is supported by a thermally conductive plate (made of metal) that provides the electrical connection between the P and N blocks;

Precisely because in the Peltier cell the P-doped and N-doped parts are not facing each other, the depletion region is not formed; this means that the junction forming the Peltier cell is not rectifying, in the sense that, unlike the PN junction diode, it conducts not in one direction but in both. Effectively, the semiconductor junction at the base of the Peltier cell is a P/metal/N structure, but it is appropriately "flipped" to create a geometry that allows for many of them to be mounted, electrically connected in cascade or in series and parallel. Moreover, the adopted shape allows exposing the junction so that its temperature and temperature difference can be perceived. The elementary junction forming the Peltier cell (Figure 2.1) is composed of a piece of N-doped silicon (with pentavalent impurities, therefore electronically negative) and another doped with P (with trivalent impurities, therefore electronically positive) placed side by side and welded together, with the interposition of metal; however, this is not like traditional ones because the contact point between the N-type silicon part and the P-type silicon part is made

by a metal foil. By applying a positive potential difference to the free ends of this elementary junction on the P-doped region and negative on the N-doped region, the outer surface (i.e., the free one) of the former becomes cold and that of the latter as well; instead, the metal electrode connecting the two semiconductor pieces heats up. By reversing the polarity, the metal part cools down and the outer P and N regions heat up.

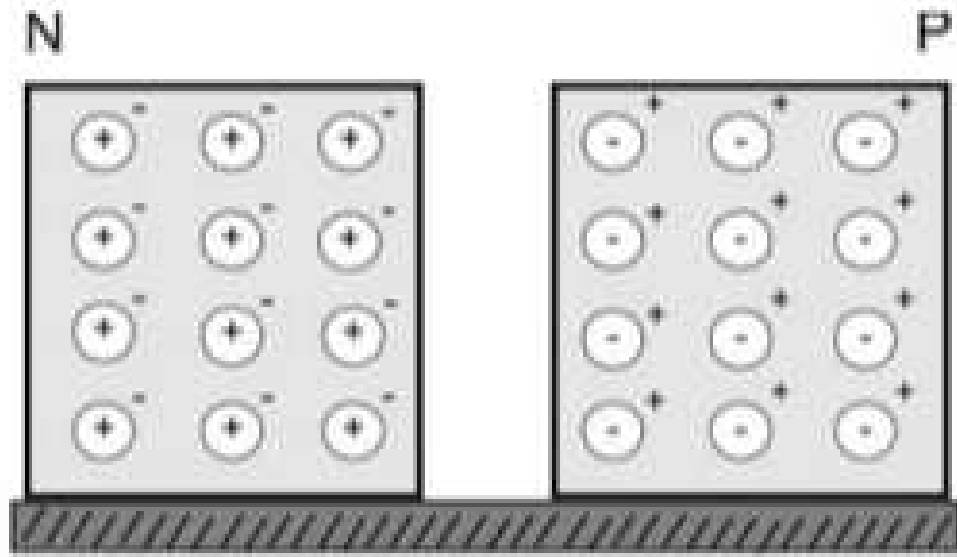


Figure 2.1: P-N Junction

Therefore, the following general rule applies:

- The P-doped semiconductor (thus poor in electrons available for conduction) heats up on the side from which the current exits and cools down on the side where the current enters.
- The N-doped semiconductor (rich in electrons available for conduction) heats up on the side from which the current enters and cools down on the side from which the current exits.

Chapter 3

Peltier Cell

After considering the physical laws that determine the basic principles of the Peltier cell and reviewing the semiconductor theory applied to the cell, let's now analyze in detail its structure, formulas, and applications.

3.1 The structure of the semiconductor Peltier cell

The actual semiconductor Peltier cell resembles the structure formed by metals, so it consists of three blocks with alternating polarity: P-N-P or N-P-N. The junctions created between the differently doped semiconductor pieces are not rectifying because they are obtained by soldering the various blocks onto metal strips, thus the typical potential barrier of the junction explained in previous sections is not formed. Therefore, the Peltier cell underlying the commercially available thermoelectric modules has a basic structure exemplified in Figure 3.1 and consists of two soldering joints or unions between semiconductors with different doping. A quick look reveals how the opening of the joints and the resulting arrangement are made so that during use, the heating zones are all on one side, and the cooling zones are on the opposite side. Specifically, during use, the P-N junctions where the current exits from the P region to enter the N region will become hot, and the N-P junctions where the current enters the P region will also become hot.

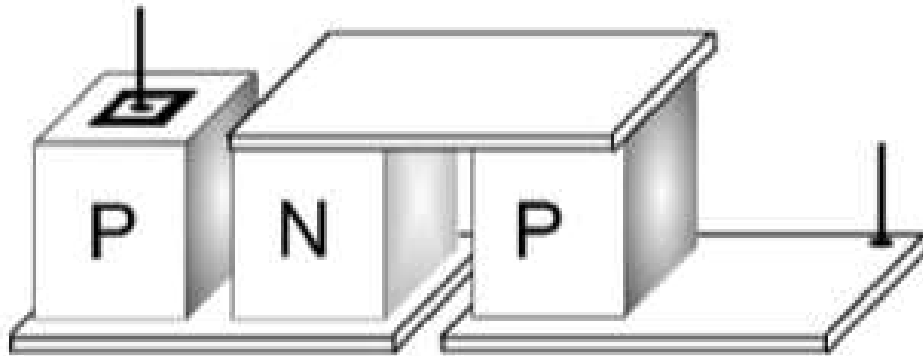


Figure 3.1: P-N Junction on Peltier Cell

The thermal behavior of the semiconductor Peltier cell is explained by considering again the thermoelectric effect and, more generally, what happens in metals as temperature increases. As mentioned in the previous pages, the outer electrons of metals are weakly bound to the nuclei of the corresponding atoms. Therefore, if they receive energy (e.g., in the form of heat), they "vibrate" more, which can be understood as them jumping to the surface and then returning inside, attracted by the nuclei. Bringing the discussion back to the P-metal-N-metal-P structure, when both soldering joints (metal strips) are at the same temperature, the potential difference between the P-type semiconductor and the N-type semiconductor (negative on the latter) is compensated by the opposite potential difference due to the soldering between the N-type and P-type semiconductors. However, heating only one of the soldering joints causes an imbalance, and one of the two potential differences predominates, resulting in a real electric tension at the ends of the group, amounting to a few mV. This corresponds to the manifestation of the Seebeck effect in the semiconductor structure. Viewing the phenomenon in reverse, i.e., analyzing the system from the perspective of the Peltier effect, it can be observed that in a structure composed of two types of semiconductors, a higher density of electrons on one side compared to the other causes a temperature difference. Specifically, where there are more electrons, more heat is produced due to the energy possessed by each electron, while on the side from which electrons are subtracted, the temperature decreases. Therefore, by supplying power to the P-N-P structure shown in the previous figure 3.1 so that the P-type region on the left is positive relative to that on the right, the lower zones become hot and the upper zone becomes cold (Figure 3.2); conversely, by polarizing the Peltier cell so that the current enters from the P-doped semiconductor block on the right and exits from the one on

the left, the upper metallic part becomes hot and the lower parts become cold (Figure 3.3). The discussion about current may seem contradictory because, as

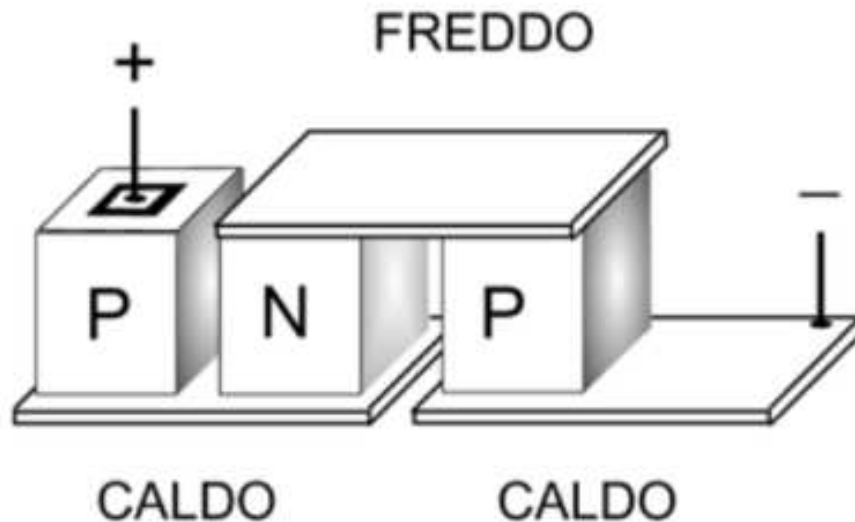


Figure 3.2: P-N Junction - When current enters the P-type region on the left and exits from the right, the junctions at the top cool down while those at the bottom heat up.

just explained, the N-doped semiconductor heats up on the side where it receives current, while the P-doped semiconductor does so on the opposite side. However, there is no contradiction because in reality, things work in reverse: the conventional direction of current is from the positive pole to the negative pole of the generator, but electrons, and thus the actual electric current, flow in the opposite direction. Therefore, as taught in Electrical Engineering, the actual direction of the current is opposite to the conventional one and flows from negative to positive. Referring to the usual figure 3.1, when the positive pole is applied to the P-region on the left, electrons accumulate on this electrode, causing the P-region where the current conventionally enters to cool down. This cooling effect is more pronounced closer to the positive electrode, which attracts all the electrons, allowing the region to cool down. On the other side, the negative pole continuously emits electrons directed towards the positive pole. Therefore, the P-region receiving these electrons becomes enriched and heats up due to the electronic activity and continuous recombination of negative charges releasing energy as they fall into the holes (electron deficiencies typical of a semiconductor doped with trivalent impurities). As for the N-doped regions, the behavior is specular: if they receive electrons from the negative pole of the generator or from a P-region, they tend to heat up, especially closer to the

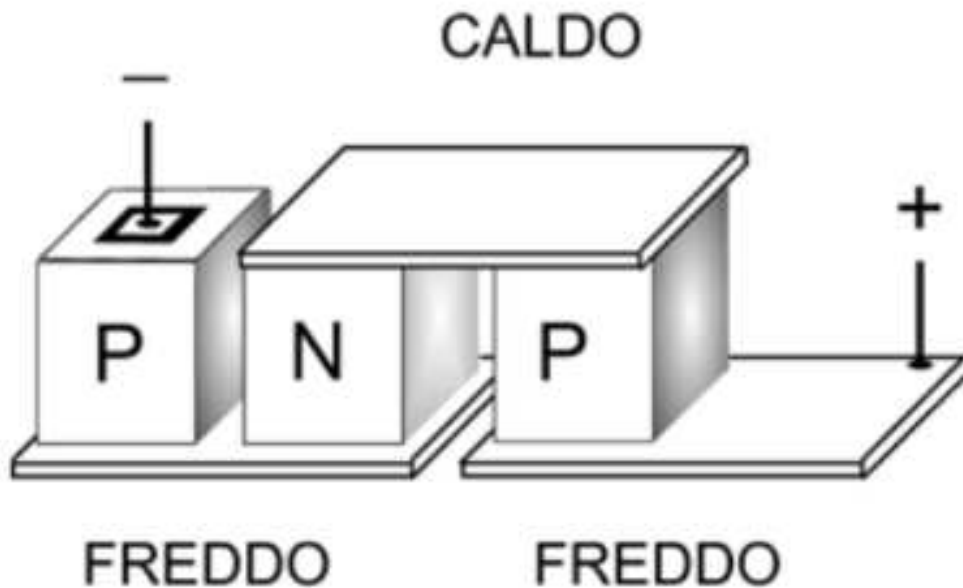


Figure 3.3: P-N Junction - When current enters the P-type region on the right and exits from the left, the junctions at the top heat up while those at the bottom cool down.

negative pole or the aforementioned P-region. However, if they lose electrons due to the proximity of the positive pole of the generator or the P-region toward which the polarization pushes the negative charges (electrons), they cool down. This cooling effect occurs because they do not recombine, retaining their energy and not releasing heat; instead, they absorb heat.

3.2 Thermoelectric modules (TEC)

In practical applications, a single P-N-P structure alone doesn't serve much purpose. Similar to analyzing the traditional bar formed by three portions of metal welded together, the potential difference achievable from a single cell is negligible, as are the amount of heat and the temperature differential (temperature difference between the hot and cold side) achievable. To overcome these limitations, composite structures are created by placing many elementary cells in series (Figure 3.4). This way, a voltage easily obtainable from a stabilized power supply can be applied to the system (the few tens of millivolts supported by a basic cell would hardly be

controllable with a traditional circuit).

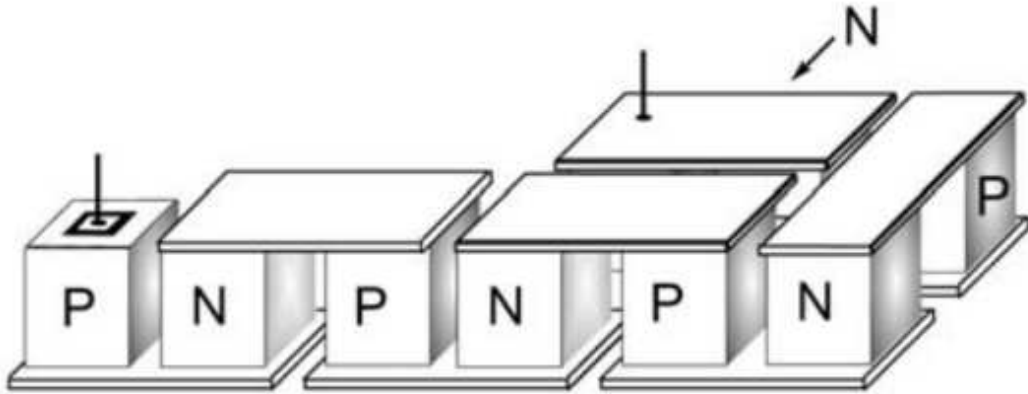


Figure 3.4

That's why those components available in the market under the name of Peltier cells are actually composed of many small cells connected to each other in series and parallel. But how is the connection made? It's simple: each copper strip connects a P-region and an N-region, and the connection is made to ensure that the strips at the top always carry the current from the P-region to the N-regions if the applied polarity is positive at the entrance of the first P-silicon region, or vice versa if the voltage applied to the cell is positive at the entrance of the first N-silicon region. In other words, during construction, the semiconductor parts are organized and arranged so that their connections allow the current to flow in the same direction for each N-region and likewise for the P-regions. Typically, to increase the cooling power and overall working capacity of industrially produced cells, a series-parallel connection is preferred: strips consisting of individual P-N-P (or N-P-N) single cells are connected in cascade, meaning the P-region of the previous one is electrically connected to the N-region of the next one (which will therefore be of the N-P-N type). Then, the ends of the individual strips are connected together in parallel. It should be noted that the connection is made so that the ends are distinguished by polarity, meaning if a strip begins with a part of semiconductor with P-type doping, it should be connected to the terminal P-part of the others, and vice versa for the end. To hold together the various parts, an alumina plate is glued on top of the metal plates; the same operation is repeated on the opposite side, thus creating a wafer structure (or a sandwich, if you prefer...) as shown in Figure 3.5.

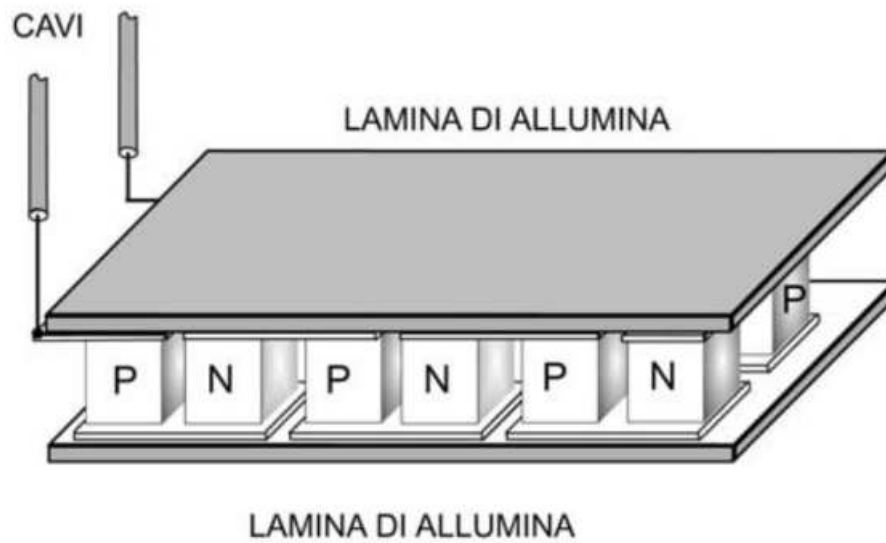


Figure 3.5: TEC Structure

The bonding is carried out using adhesives capable of withstanding temperatures of several tens of degrees Celsius without deforming or softening, such as epoxy resins. It should be noted that in many commercially available cells, one of the two sides of the alumina plates is coated with a copper foil; this precaution is adopted on what the manufacturer designates as the hot side, i.e., the side that will be the hot side during normal operation. The alumina plate is on the cold side, and the addition of the copper-coated surface serves primarily to improve heat transfer and its dissipation through the heatsink. However, it should be remembered that since Peltier cells are reversible, speaking of a hot and cold side only makes sense when they are operating; theoretically, the cold side can become hot and vice versa, as the cooling and heating sides depend on the direction of the current powering the device. Reversing the polarity and thus the direction of the current reverses the situation.

3.3 Electrical connections

The series-parallel connection of Peltier cells in industrial thermoelectric modules (TECs) allows for devices to operate at voltages easily obtainable from stabilized power supplies, with voltage differences ranging from 5 to 20 volts. Additionally, it ensures a much greater temperature difference (thermal gradient) between the hot and cold sides than what a single cell could produce and enables the development of a significant thermal (or refrigeration) power. Typically, commercially available

Peltier cells allow for theoretical temperature differences between the hot and cold sides of up to 70°C . However, in practice, this usually does not exceed 50°C . Peltier cells commonly used for cooling and heating have these parameters. Nevertheless, in recent years, the industry has begun to produce thermoelectric modules capable of withstanding more intense thermal excursions, designed for energy harvesting and thermoelectric power generation applications. Usually, Peltier cells have power cables (two, at the ends of the series of elements that compose them) color-coded, meaning one is red and the other is black; they have a polarity. At this point, one might wonder why, given that the cells are actually reversible, it makes sense to attribute a polarity to the connections. The answer is simpler and more straightforward than it seems: supplying a positive voltage on the red wire relative to the black wire, the cell cools on the natural alumina side and heats on the copper-coated side; this results in optimal operation because the heat sink is applied to the copper-coated side. It is entirely possible to do the opposite, but the thermal resistance of the cold side is theoretically slightly higher than that of the copper-coated side, resulting in slightly lower performance. For cells that have both sides made of the same material, polarity may not be considered, and the wires can be interchanged if needed. In reality, indicating the polarity of the connections primarily ensures that the side identified as hot by the manufacturer, when polarizing the thermoelectric module with positive polarity on the positive wire, heats up, while the side identified as cold becomes cold, always applying voltage with the same polarity.

3.4 Application

The capability of Peltier cells to generate cold enables the use of these devices in numerous applications where targeted refrigeration is required, especially in small spaces where traditional compressor-based refrigeration systems using gas or ethylene glycol (or ammonia) are not feasible. They are also used in applications requiring rapid and easily modulated freezing or cooling, which only Peltier cells can provide. Specifically, Peltier cells are used for:

- Creating coolers to be mounted in environments where the presence of vibrations and mechanical stresses discourages the use of traditional air conditioners and refrigerators.
- Cooling solutions in chemistry and physics laboratories, rapidly lowering the temperature of various products (always in a scientific context).
- Cooling biological compounds in analysis laboratories.
- Operating rooms, to keep biological compounds, blood, tissues, or organs for transplantation cool or to cool them.

- Aesthetic dermatology, in combination with pulsed light laser, where they are used to cool the skin after laser application, to protect the patient's skin and reduce the sensation of heat.
- Cooling electronic components such as CPUs, both for direct application and through liquid circulation systems.

In all applications, to achieve the desired cold, it is necessary to implement a static system (with convection heat sink) or dynamic system (with fans or liquid circulation) to remove the heat accumulated from the hot side. Simply powering the cell is not enough; it is essential to maintain the temperature differential through appropriate measures for the application. This is because, while the electric current determines the cooling of one side, the opposite side heats up, and it is necessary to lower its temperature to keep it below a certain limit to prevent device damage. By manipulating the temperature differential, greater cooling of the so-called cold side can be achieved. Furthermore, since the temperature of the cold side depends directly on that of the hot side under the same applied voltage and current, cooling the hot side further enhances the cooling capacity of the Peltier cell module on its cold side.

3.5 Technical parameters

- Electrical power: It is given by the product of the maximum withstand voltage (V_{max}) and the maximum current (I_{max}) that can flow through the cell; measured in watts and referred to a temperature of the cold side equal to $27^{\circ}C$.
- Cooling power (symbol P_f or Q): It is the capacity to absorb heat from the cold side and exactly represents the thermal power that the cold side can cancel out.
- Maximum working voltage (V_{max}) with the cold side at $27^{\circ}C$, expressed in volts (V).
- Maximum working current (I_{max}) with the cold side at $27^{\circ}C$; expressed in amperes (A).
- Temperature difference (δt): It is the maximum temperature difference between the cold and hot sides (also known as thermal gradient).
- Maximum temperature on the hot side: It represents the limit temperature that the hot face of the cell can reach.

3.5.1 The thermal gradient

For each manufactured cell, the manufacturer specifies the achievable temperature difference between the hot and cold sides, often referred to as the thermal gradient; this parameter allows the designer to get an idea of what they can expect from their cell. The thermal gradient is referenced to the maximum developable power but is theoretical, so it depends on various factors. The temperature difference between the hot and cold sides is a function of the current passing through the component; theoretically, it could be unlimited. However, in practice, this is not the case, and there are two factors at play: first, the thin semiconductor thickness propagates heat towards the cold side, preventing a thermal gradient exceeding 40°C; secondly, as the current in the cell increases, so does the power and therefore the heat dissipation. Thus, to effectively cool the cold side, the heat produced by the cell when operating near its maximum power must be dissipated, otherwise the heat from the hot side will be absorbed by the cold side. The radiator or other heat dissipation system must therefore be sized based on the temperature at which the hot side of the Peltier cell is to be maintained and the thermal power to be dissipated from the hot side.

3.6 Dissipating the heat from the hot side

In the case of conductors or semiconductor electronic devices, including Peltier cells, this heat is partially absorbed by the cold side (due to the inevitable thermal conductivity of the material used) and largely dissipated into the surrounding environment. The greater the portion dissipated into the environment compared to what ends up on the cold side, the greater the thermal gradient made possible by the use of the Peltier cell. To understand how heat is dissipated, one can hypothesize that the electrical power to be dissipated is analogous to an electrical current flowing under the influence of a temperature difference, which can be considered as a voltage. Imagining that the temperature difference (referred to here as 'T) between the hot side of the cell and the environment in which the component must operate is a potential difference, one can define a thermal resistance as the obstacle encountered by heat in propagating. Therefore, in analogy with Ohm's Law, one can write:

$$R = \frac{V}{I} \quad \theta = \frac{D_T}{P_D}$$

The parameter θ symbolizes the thermal resistance, which is the resistance that heat encounters when exiting the junctions of the cell to disperse into the environment; the lower θ is, the more power the component can dissipate, given the same ambient temperature and maximum temperature tolerance of the semiconductor. In the

case of Peltier cells, the maximum allowable temperature on the hot side is defined by the manufacturer to avoid semiconductor damage; typically, this value ranges between 60 and 75 °C. The manufacturer also defines the thermal resistance of the component. From the formula, it is noted that the thermal resistance is expressed in degrees Celsius per watt $\frac{^{\circ}C}{W}$; the higher the thermal resistance, the more heat is retained by the cell, given the same ambient temperature, and consequently, the higher the temperature on its hot side and, consequently, on its cold side. Conversely, the lower this resistance, the easier it is to cool the hot side. Pd is the electrical power that the cell must dissipate; the maximum is typically defined by the manufacturer. In all cases, it should be remembered that power is derived from the relationship:

$$P_D = V * I$$

where V is the voltage applied to the Peltier cell and I is the current it absorbs; **Example:** consider using a cell manufactured by Marlow Industries that can dissipate a maximum of 42 W, withstand a voltage difference not exceeding 8.1V, and absorb a maximum current of 5.3 A. According to the specifications, the component allows a hot-side temperature not exceeding 67 °C. With these parameters known, the thermal resistance can be determined, assuming the cell is powered with 8 V, at which it absorbs approximately 5 amperes; the dissipated power is:

$$P_D = V * I = 8V * 5A = 40W$$

Given the Pd, assuming an ambient temperature of 30°C, we can substitute the known parameters into the formula for thermal resistance and calculate θ .

$$\theta = \frac{D_T}{P_D} = \frac{(67 - 30)^{\circ}C}{40W} = 0.925 \frac{^{\circ}C}{W}$$

Therefore, the thermal resistance physically existing between the junctions of the hot side of the Peltier cell in question and the surrounding environment must be 0.925 $\frac{^{\circ}C}{W}$ or less. It is worth noting that typically a Peltier cell does not operate alone but is cooled using a simple radiator or a liquid cooling system; in all cases, the thermal resistance calculated using formula (I) represents the combination of multiple resistances, one due to the cell structure, another to the coupling between the hot side and the heat dissipation system, and the last one between the heat dissipation system and the surrounding environment.

3.7 Benefits of thermoelectric generators

"Thermoelectric modules manifest some advantages when the other harvesting methods and sources of energy coming from the environment are considered. First

of all, thermoelectric generation is some kind of solid state power conversion. Therefore the Peltier devices do not have any moving parts, so they are reliable, silent and they are characterized by very long MTF (mean time to failure). Moreover they are not chemically hazardous. Next, opposite to photovoltaic panels they can operate in conditions where there light is not sufficient or not available at all. Finally, temperature gradients have tendency to change rather more slowly than the amplitudes of vibrations which often are occurring as single bursts. Therefore, thermoelectric generators can provide energy in a continuous way"^[3].⁴

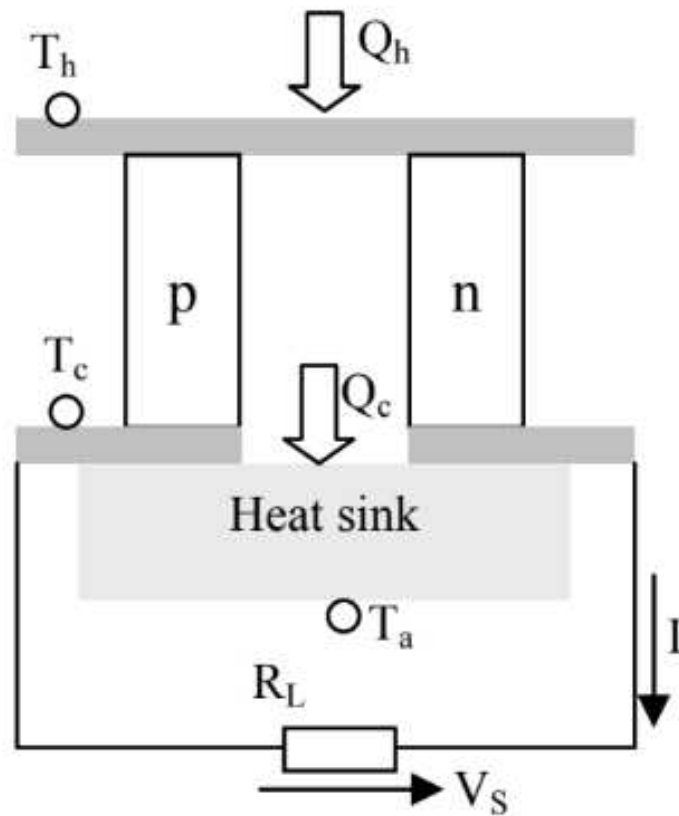


Figure 3.6: Heant Sink

⁴Modeling and Simulation of Thermoelectric Energy Harvesting Processes

3.8 Static cooling systems

The simplest way to get rid of heat is to place the hot side on a heat sink, which is a device made of high thermal conductivity metal (such as pure aluminum or copper, for example, which are metals that present the lowest thermal resistance at the same cost) that allows heat to flow away and dissipate easily into the surrounding air. In order to achieve this, in addition to being composed of material with low thermal resistance, the radiator has a considerable surface area, which is extended by giving it particular shapes with various fins arranged along a precise direction, allowing it to benefit from any air currents. Heat sinks are available in various types and shapes, already cut or sold in bars; for each one, the manufacturer defines the overall thermal resistance or the specific resistance per unit of linear measurement (for example, $1\text{ }^{\circ}\text{C}$ every half meter). In summary, the thermal resistance of a Peltier cell should be seen as the combination of two resistors, one represented by the resistance between the semiconductor and the hot side (θ_{jc}), and the other by the resistance between the aforementioned hot side and the environment (θ_{ca}); the latter is usually divided into two parts because adding the heat sink results in the combination of the thermal resistance between the container and the radiator and that between the radiator and the environment.

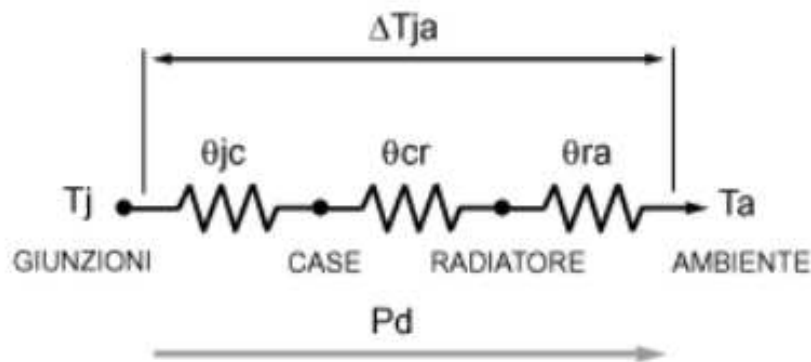


Figure 3.7: Termic Resistance

In summary (Figure 3.7), the cell/heatsink system consists of three thermal resistances, namely θ_{jc} (junction-to-case resistance), θ_{cr} (case-to-radiator resistance), and θ_{ra} (radiator-to-ambient resistance). The three resistances are in series with each other and therefore all experience the same power (P_d) or heat flux; each of them exhibits a temperature difference directly proportional to its value across its virtual terminals, and together they result in a drop equal to that between the junctions and the ambient (θ_{ja}).

3.8.1 Dissipator Calculate

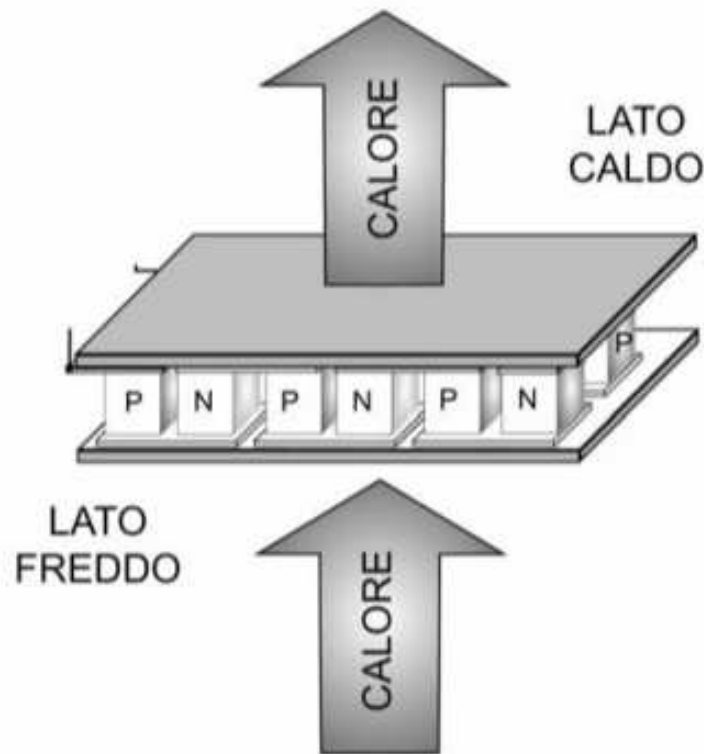


Figure 3.8

Now let's see how to calculate the conventional radiator. Considering the diagram shown in Figure 3.8, we start by obtaining the overall thermal resistance, obtained by dividing the difference between the maximum semiconductor temperature (θ_{jMAX}) and the ambient temperature by the power to be dissipated (P_d):

$$\theta = \frac{D_T}{P_D} = \frac{(\theta_{jmax} - \theta_a)}{P_D}$$

Resuming the example of the Marlow Industries cell with 42 watts powered at 8 V and 5 A, knowing that it must dissipate 40 W and imposing an ambient temperature up to a maximum of 30 °C, we have the following usual parameters:

$$\theta = \frac{D_T}{P_D} = \frac{(T_{jmax} - T_a)}{P_D} = \frac{(63 - 30)^\circ C}{40W} = 0.925 \frac{^\circ C}{W}$$

Since the obtained θ is the sum of all thermal resistances, we can obtain only θ_{ra} , i.e., the thermal resistance of the heat sink, from the following relationship:

$$\theta_{ra} = \theta - \theta_{jc} - \theta_{cr}$$

The thermal resistance between the container (θ_{cr}) and the radiator depends on several factors, primarily the type of coupling and the structure of the hot side plate. However, typically, in the case of direct contact, by interposing a layer of silicone paste that improves heat transfer (by compensating for surface roughness), less than $0.1 \frac{^{\circ}\text{C}}{\text{W}}$ can be achieved. In practice, by placing the entire surface of the hot side on a well-smoothed radiator and spreading silicone-based thermal paste (usually used for power transistors or CPU heatsinks in computers), this thermal resistance can be considered negligible. As for the resistance between the junction and the container (θ_{jc}), it depends on the intrinsic characteristics of the cell. Typically, it is very low because the contact between the semiconductor junctions and the alumina is good, and alumina (ceramic) has excellent thermal conductivity. In general, the junction-to-container thermal resistance (θ_{jc}) can also be considered negligible, amounting to less than $0.1 \frac{^{\circ}\text{C}}{\text{W}}$. Given this, the sum of θ_{jc} and θ_{cr} amounts to just $0.1 \frac{^{\circ}\text{C}}{\text{W}}$. Now, let's consider mounting the Peltier cell without interposing anything other than the silicone paste. Given the sum of θ_{jc} and θ_{cr} ($0.1 \frac{^{\circ}\text{C}}{\text{W}}$), we can calculate θ_{ra} using the same approach as before for the 42-watt cell:

$$\theta_{ra} = \theta - \theta_{jc} - \theta_{cr} = 0.952 - 0.1 = 0.852 \frac{^{\circ}\text{C}}{\text{W}}$$

The radiator must therefore have a thermal resistance equal to or less than $0.825 \frac{^{\circ}\text{C}}{\text{W}}$.

3.8.2 The practical use of cells

To fully exploit the cooling capacity of the Peltier thermoelectric module, some simple rules must be followed:

- Separate the environment facing the cold side from where the heatsink radiates the heat extracted from the cell as much as possible.
- Insulate the edge of the cell with a gasket made of material that does not conduct heat (e.g., rubber, polyurethane foam, unexpanded polystyrene) from the heatsink to the cold side plate; the material used must withstand temperatures of around 80 °C without excessive deformation.
- Place a metal plate with high thermal conductivity and a very large surface area on the cold side, while interposing the usual silicone-based paste to

improve heat transfer. The plate should be at least as large as one side of the space to be cooled.

- If, as is almost always the case, the thickness of the insulation used to separate the cold zone from the hot one is greater than that of the Peltier cell, to have a large cold plate, it must be spaced from the cold side using a parallelepiped of metal, also with high thermal conductivity (e.g., copper), as shown in Figure 3.9.

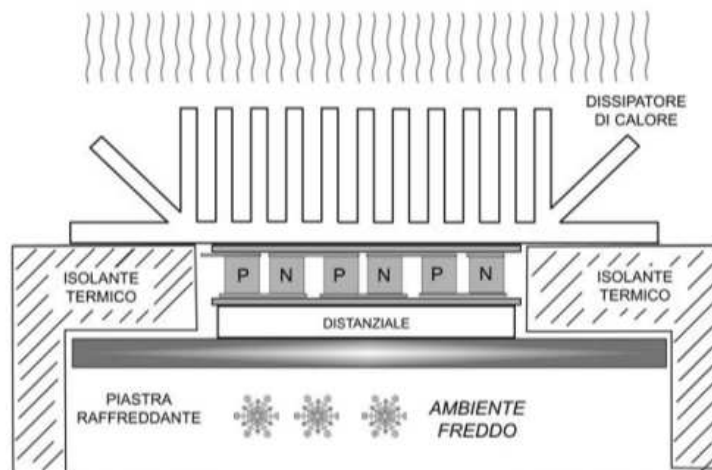


Figure 3.9: Cross-sectional area

Regarding the metal plate responsible for producing cold in the environment to be cooled, some considerations need to be made. The best option is certainly copper, unless one seeks among noble metals (silver, gold, platinum). However, its use is limited by a fact: when cooling a closed environment with a certain level of humidity, liquid condensation occurs on the cold side of the cell, which is almost always water. The issue of humidity condensation should be taken into account in other applications as well and is not relevant solely for the contamination of the cooled environment. In fact, the condensation that occurs on the cold side when the Peltier cell is used in a refrigeration system creates water that can penetrate the structure of the thermoelectric module over time. This water can oxidize the metal used for solder joints, creating problems. To avoid such problems, it is advisable to apply a seal on the edges of the cold side that occupies the smallest possible surface area but ensures the necessary seal to prevent water from entering the lattice of cells between the alumina plates containing the Peltier cells. The application of a seal slightly worsens the heat absorption by the cold side, but it is a price to pay to avoid the degradation of the thermoelectric module. Seals are usually made of

rubber or silicone, with silicone being able to improve heat transmission compared to traditional rubbers. Gelatins like those used to couple power electronic devices to heat sinks or gray Teflon seals (used to couple electronic components to their heat sinks) can also be used. Another solution is to silicone the perimeter of the cold side without touching the surface in contact with the cooling metal plate: in practice, the silicone or sealant used can be applied laterally.

3.8.3 Damage due to condensation

Condensation on the cold side of Peltier cells poses problems not only when the cells are used to cool electronic devices. While it's true that a circuit in operation, powered and wet, can suffer irreversible damage (and become dangerous), the water introduced into the thermoelectric module can also lead to cell alterations and permanent degradation. Studies and analyses on systems equipped with Peltier cells have identified two main issues: those caused by the presence of water when the cells are powered, and those due to oxidation. In the first case, there is cross-current (cell short-circuiting) which causes the exclusion of other cells. While it absorbs the entire nominal current, it loses efficiency and cools less. In the second case, the accumulation of water when cells are off causes oxidation of the semiconductor junctions and solder joints. This leads to an increase in electrical resistance over time. In the first thermal jump (deterioration of module efficiency), while in the second, the thermal jump decreases proportionally to the absorbed current (therefore, the efficiency remains almost constant, but the module does not provide the expected cooling power). Another phenomenon that can occur if water is introduced into the internal structure of the thermoelectric module, between the cells when it is powered, is electrical erosion of the metal parts of the cells, caused by electrolysis. This erosion can cause both a decrease in the contact surface in the junctions and therefore an increase in module resistance (resulting in a reduction in cooling power and electrical power absorbed), and the build-up of metal where it should not be present, with the consequent short circuit or bypass of cells or parts thereof inside the module. For all these reasons, it is advisable to have a gasket between the cold side and the cooling plate that provides a good seal, and to adopt suitable structures and channeling to remove condensed water, taking into account the inclination and possible slope of the thermoelectric modules. As mentioned, rigid sealants and adhesives should be used as little as possible and always in conjunction with modulated power supply (PWM or proportional DC) of the modules, to minimize thermal deformation and limit the onset of cracks or detachment. It is better to use soft rubber gaskets suitable for cold conditions (bearing in mind that rubber tends to stiffen and break in severe cold) or silicone gaskets.

Chapter 4

Energy Harvesting

Energy Harvesting, also known as Power Harvesting or Energy Scavenging, is the process of capturing and storing small amounts of energy from the surrounding environment to power electronic devices or systems. This approach is particularly useful in situations where it might be difficult or inconvenient to use conventional power sources such as batteries or electrical outlets. Energy harvesting technologies can convert various forms of energy, such as solar light, heat, vibrations, and mechanical motion, into electrical energy. Here are some common forms of energy harvesting:

- **Solar Energy Harvesting:** Photovoltaic cells (solar panels) capture sunlight and convert it into electrical energy. This is commonly used in solar-powered calculators, outdoor sensors, and even some wearable devices.
- **Thermoelectric Energy Harvesting:** Thermoelectric generators (TEGs) can convert temperature differences between two surfaces into electricity. For example, waste heat from industrial processes or the human body can be converted into energy for low-power devices.
- **Kinetic Energy Harvesting:** Devices like piezoelectric generators or electromagnetic generators can capture energy from vibrations, motion, or mechanical impacts. They are often used in self-powered sensors, wearable technology, and high-efficiency lighting systems.
- **Radio Frequency (RF) Energy Harvesting:** RF scavenging technology captures and converts electromagnetic energy from sources like Wi-Fi signals, cellular networks, and RFID readers into electrical energy. It can be used to extend the life of small, low-power devices.
- **Wind Energy Harvesting:** Small wind turbines or micro wind generators

can capture energy from air movements or wind and convert it into electricity for various applications, including remote sensors and communication equipment.

- **Vibration Energy Harvesting:** Devices like piezoelectric materials or electromagnetic generators can capture energy from vibrations in machinery, vehicles, or other mechanical systems.
- **Hydrokinetic Energy Harvesting:** Devices placed in flowing water, such as rivers or streams, can harness the kinetic energy of water movement to generate electricity.

Energy harvesting technologies have gained importance in recent years due to the increasing demand for autonomous and low-maintenance electronic devices in fields such as the Internet of Things (IoT), remote monitoring, and wearable technology. While energy harvesting solutions provide a way to reduce reliance on batteries and extend the operational life of such devices, they are often limited by the available energy source and the efficiency of the harvesting technology. Design considerations, such as energy management, storage, and high-efficiency components, are essential to make energy harvesting systems practical and effective.

Table 4: Summary of different types of energy converters.

Harvester type	Output voltage	Power density	Efficiency	Notes ^{a)}
Photovoltaic	Typically 0.7 ± 1.5 VDC per module. Up to 2.5 VDC per module in multijunction devices [5].	15 mW/cm ² [1] 10 mW/cm ² , 10 μ W/cm ² in indoor lighting [51, 52]	Highest: $32.0 \pm 1.5\%$ Typical: $25.0 \pm 1.5\%$ [5]	+ Direct DC voltage easy for energy management hardware – Amount of light might be insufficient • Commercially available
Thermoelectric	Up to 10 VDC with commercial modules ^{b)} [16–18].	Up to 10 mW/cm ² [7]	2.70 – 5.02% ^{c)} 3% [51]	+ Direct DC voltage easy for energy management hardware • Commercially available [16–18]
Piezoelectric	2 – 10 VAC [24]	250 μ W/cm ³ [41] 330 μ W/cm ³ [1] ^{d)}	^{e)}	+ Relatively high output voltage – Typically very high output impedance, > 100 k Ω [20] • Commercially available [29–31]
Electromagnetic	< 1 VAC [20] 0.1 – 0.2 VAC [41] Typical values for commercial harvesters are up to 10 VDC ^{f)} [35, 37].	^{d)}	^{e)}	– Low output voltage difficult for energy management hardware • Commercially available [35, 37] • Relatively high output current levels achievable at the expense of low voltages [20]
Electrostatic	2 – 10 VAC [24] ≥ 250 VAC [40]	50 μ W/cm ³ [41] ^{d)}	^{e)}	+ Easiest to integrate in MEMS systems [41] – Separate voltage source and mechanical stops needed [24] – The output impedance is often very high [20] • At research stage, no commercial solutions available
RF	3.3 – 5.25 VDC (commercial harvesting modules) [50]	GSM 900/1800 MHz: 0.1 μ W/cm ² WiFi 2400 MHz: 0.01 μ W/cm ² [51]	50% ^{g)} [7, 50]	+ Energy can be harvested from ambient electromagnetic radiation, – but the power density is very low – Higher power density can be achieved with external RF transmitter [7] • Commercially available for 915 MHz (ITU region 2, North and South America) [50]

a) + Advantage, – Disadvantage, • Other notable issue

b) Depends on the number of the thermoelectric couples in module, and the temperature gradient.

c) Commercial thermoelectric modules reported in this work.

d) Mitcheson et al. [2] state, that power density provides a meaningful comparison only in situations when the source characteristics are fixed

e) Max power, and therefore the efficiency, is source dependent

f) Commercial electromagnetic harvester modules include energy management hardware. The size is also a notable issue.

g) Efficiency of the harvester itself, excluding transmission efficiency.

Energy Source	Conversion Devices	Outlook
Radio Frequency	Antenna	Low loss power transfer, efficient at centimeter scale antenna efficiency drops steeply sub-mm
Optical	Photovoltaic Cell	Efficient and high scalable, requires line of site access to light source
Mechanical	Piezoelectric	Wide range of source availability over range of frequency, high efficiency for biological systems, challenges in scaling mechanical structures at sub-mm scale
Thermal	Thermoelectric	Waste heat available in many situation, thermoelectric behavior scalable but requires temperature gradient, challenges in scaling radiative approach
Nuclear	Betavoltaic	Scalable with long-term stable source, challenges in scaling ensuring health and safety and scaling packaging
Chemical	Chemical Cell	Can utilize energy sources in specialized environments, drawbacks of long time constant or startup time and scaling reactor chambers to sub-mm dimensions

Table 4.1: Summary Application

Chapter 5

Lithium Battery

In this chapter, we will discuss the battery, particularly the lithium-ion battery: its composition, chemical-physical properties, uses, criticalities, but above all, how to elaborate the State of Charge (SoC). This is because the device we will discuss in the following chapters is powered by this type of battery, and before understanding how the Peltier cell must be set to power this battery, we need to have an idea about the components we are going to use.

5.1 Chemical Composition

In this chapter, we will provide an overview of various types of lithium-ion batteries and their characteristics. Subsequently, we will delve into aspects related to the control and management of cells, including the functionalities that a Battery Management System (BMS) must implement.

5.1.1 Lithium-ion Battery

In recent years, lithium-ion batteries (Li-ion) have gained ground in high-power applications such as electric or hybrid vehicles (EVs, HEVs) and smart grids. This technology has become prominent due to significant advantages over batteries based on different chemistries such as nickel-cadmium (Ni-Cd), nickel-metal hydride (Ni-MH), and lead-acid. Lithium-ion cells consist of a cathode composed of a metal oxide and a porous carbon anode separated by an electrolyte responsible for ionic conduction. Lithium ions move between the electrodes (Figure 5.1), with the direction determined by whether the battery is discharging or charging. This movement of ions gives rise to the term "rocking chair" for lithium batteries. The characteristics of each lithium cell are determined by the material composing the cathode, with the exception of lithium titanate batteries, which use lithium titanate

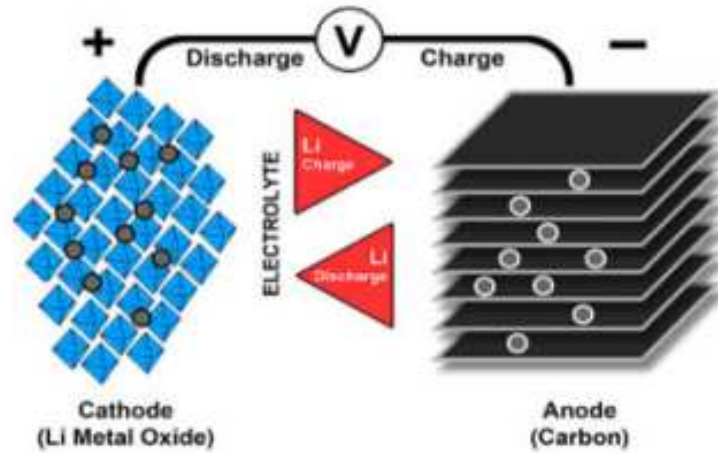


Figure 5.1: Basical Principle

as the negative electrode material. The main materials used for the cathode are: cobalt oxide (LiCoO_2 , LCO), manganese oxide (LiMn_2O_4 , LMO), iron phosphate (LiFePO_4 , LFP), and nickel-manganese-cobalt oxide ($\text{LiNi}_{1-x-y}\text{Mn}_x\text{Co}_y\text{O}_2$, NMC). A comparison between these types is illustrated in Table 5.1.

Value	LCO	LMO	LFP	NMC
Voltage	3.9	3.7	3.2 - 3.3	3.6 - 3.7
Cutt-off	4.2	4.2	3.6	4.2
Cycle life	500	500-1000	1000 - 2000	1000-2000
Specific Power	155	100-120	160	200
Energy	1	10-40	35	10
Thermal Escape	150	250	270	210
Security	Low	Middle	Hight	Good
Cost	Hight	Low	Middle	Hight

Table 5.1: Differences Between Battery Types

5.1.2 Disadvantages of Lithium Cells

The main drawback of lithium chemistry, compared to other technologies, is its high sensitivity to temperature and operating voltage ranges of the cell; these two

parameters need to be continuously monitored to be kept within the Safe Operating Area (SOA) of the battery. Deviation from the safety ranges can cause internal damage to the cell, leading to thermal runaway or explosion. The limits of the SOA are defined by the discharge and charge cut-off voltages and the operating temperature of each cell. Prolonged charging beyond the upper limit leads to the formation of a metallic lithium layer on the anode, while prolonged discharging can be even more damaging and result in cell short-circuiting. Regarding temperature, charging the battery below 0°C leads to the deposition of metallic lithium on the cathode surface, shortening the cell's lifespan. At temperatures above the upper limit, damage occurs to the separator between the electrodes, and lithium reacts with the electrolyte.

5.1.3 Advantages of Lithium Cells

- The strengths of lithium batteries are:
- Absence of memory effect;
- High specific power, specific energy, and energy density;
- High charging currents;
- Higher nominal voltage;
- Low self-discharge rates: approximately 5% per month compared to the 30% per month of nickel-based batteries.

5.2 Functions of a BMS

Despite the inconveniences and problems suffered by lithium batteries, their performance advantages over other chemistries make them successful for many applications. Therefore, it is worthwhile to implement the necessary functions to maintain safety and optimize the use of lithium cells. In electric or hybrid vehicles, to achieve the required voltages (hundreds of volts), many lithium cells are connected in series; this implies that the battery management circuit must deal with multi-level monitoring, from the individual cell to the entire pack.

In Figure 5.2, the main tasks that the battery control circuit must perform are schematically outlined. The essential functions are:

- **Voltage measurement:** It is necessary for each cell due to various factors such as different temperatures among the cells, module imbalance, and therefore different states of charge.

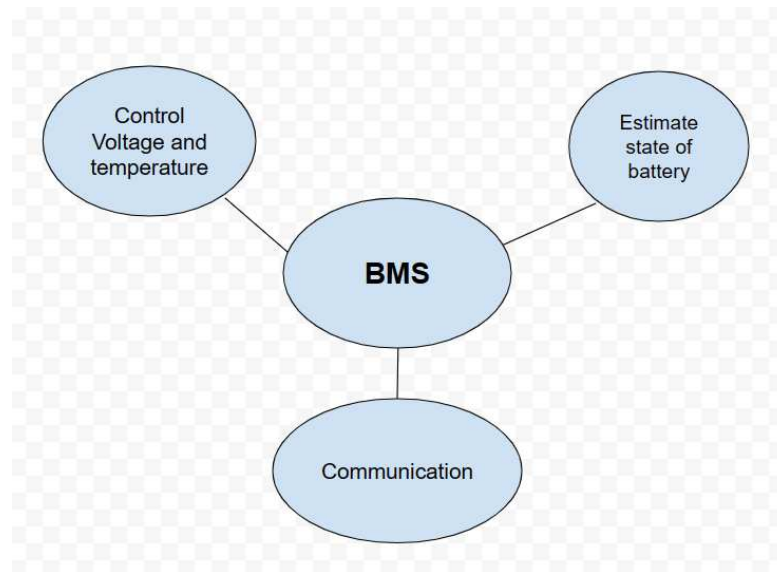


Figure 5.2: BMS Chart

- **Current measurement:** It is necessary to prevent exceeding certain maximum limits; moreover, it is fundamental for the implementation of most battery state estimation algorithms.
- **Temperature measurement:** It can be done for individual cells, but it is not necessary; the number of sensors can be limited by placing them at appropriately identified points. In addition to measuring these quantities, the BMS must be able to take appropriate control actions if they exceed the normal operating limits set by the manufacturer.

Secondary but very important functions include:

- **Battery state estimation:** It includes estimating two important parameters that are not directly measurable. The State of Charge (SoC) is an indicator of the remaining charge that the battery can still deliver, thus providing an idea of the remaining autonomy. The State of Health (SoH) is a parameter that specifies the maximum amount of charge the cell can store, which decreases during the battery's life and use.
- **Balancing:** In a battery pack consisting of cells connected in series, it is not certain that all cells have the same SoC; indeed, this condition rarely occurs because the maximum capacity (Q_{max}) is different for each cell. It becomes important to implement a charge equalization function in the battery control circuit so that the battery capacity can be maximized. In case of imbalance, the end of discharge will be determined by the least charged cell, and vice

versa in the case of charging, causing suboptimal battery usage. Balancing can be performed passively, by discharging the more charged cells to a shunt resistor, or actively, by transferring the charge from cells with higher SoC to those with lower SoC through a DC-DC converter and a switch matrix; the first solution is more economical but less energy efficient compared to the second.

- **Communication:** The BMS is often integrated into more complex systems, and it is necessary for it to be able to exchange messages and information with the user and other components of the overall system, which implies the use of a communication protocol. In the automotive environment, the most used protocol is the CAN-bus, a serial protocol particularly suitable for noisy systems. If they exceed the normal operating limits set by the manufacturer.

5.2.1 BMS Architectures

As previously stated, in high-power applications, hundreds of cells are required to reach the necessary voltages. For better battery management, the cells are hierarchically organized into modules, which in turn, when connected in series, form the pack. The architecture of the BMS depends on the application in which it is used, and a hierarchical modular structure is often adopted: there is a Cell Monitor Unit (CMU) that communicates with the Module Monitor Unit (MMU), which exchanges information with the highest level of the system, the Pack Management Unit (PMU). Communication between the various levels occurs via CAN; an example of this type of architecture is illustrated in Figure 5.3. The PMU is responsible for estimating SoC and SoH.

5.3 SoC & SoH

As mentioned in the previous chapter, one of the tasks of the BMS is to estimate the state variables of the battery. There is a wide range of such variables because, depending on the application, it may be necessary to highlight certain battery characteristics over others. In electric vehicles, for example, there is talk of State of Power (SoP) and State of Energy (SoE), necessary for regulating energy emission and recovery. In this section of the paper, the state of charge and state of health will be defined, and the algorithms that allow their estimation will be analyzed.

5.3.1 State of Charge SoC

SoC is a parameter related to the concentration of lithium in the two electrodes; it indicates the remaining charge that the battery can provide to the system it

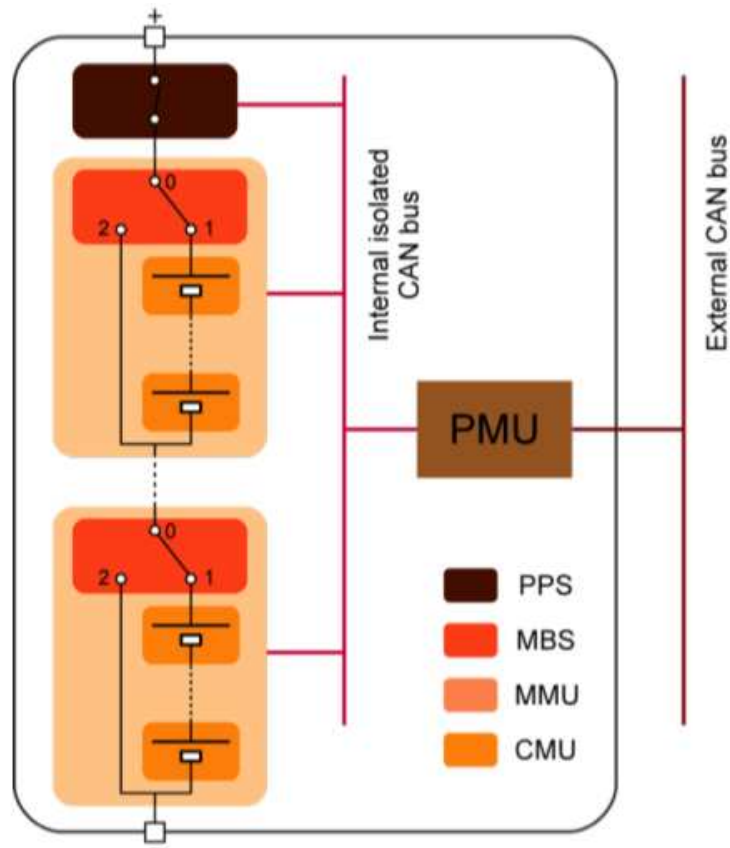


Figure 5.3: BMS Architectures

powers. Knowing the state of charge precisely allows keeping the cell within safe operating limits and provides an idea of the remaining autonomy. A common definition of SoC is the ratio between the remaining charge (Q_c) and the nominal capacity of the cell (Q_n), at ambient temperature and sufficiently low C-rate ($C = Ah$). $SoC = \frac{Q_c}{Q_n}$. This formula does not take into account cell aging, as the remaining charge is normalized to the nominal capacity; alternatively, SoC can be defined as the ratio between Q_c and the maximum charge stored, Q_{max} . If this latter definition is adopted, it should be noted that the term in the denominator varies with the cell's life.

5.3.2 Estimation of SoC: Methods

The techniques developed to obtain an estimate of the state of charge vary and are distinguished by the accuracy and computational complexity required, factors that affect the cost of the BMS implementing the algorithms. This entails choosing a

method suitable for the application and the precision it requires.

Coulomb Counting

Since the quantity of interest is charge, the most immediate idea is to integrate the current flowing through the cell over time; this technique is called Coulomb Counting and is one of the most commonly used by SoC estimators. Given $t = 0$ as the initial time, the charge at time $t = T$ will be given by:

$$Q(t) = Q_0 - \int_0^T i_L(t) dt$$

Having adopted, in this thesis work, the definition $SoC = \frac{Q_c}{Q_{max}}$, the variation over time of the state of charge, relative to the initial value (SoCinit), is calculated as follows:

$$SoC(t) = SoC_{init} - \mu_i \int_0^t \frac{i_L(\tau)}{Q_{max}} dt$$

where μ_i represents the coulombic efficiency, a parameter that takes into account the different charge transfer efficiencies between the charge and discharge phases ($\mu_i = 1$ during discharge and $\mu_i < 1$ during charge). The results obtained with Coulomb Counting can be very accurate; however, the method has some disadvantages:

- The value of SoCinit is not derived by integrating the current, but it needs to be known accurately beforehand. It is often obtained from a look-up table where samples of the OCV(SoC) characteristic are stored, where OCV (Open Circuit Voltage) is the open circuit voltage of the cell. This method of determining the initial state of charge is not accurate and causes a significant absolute error on SoC.
- The value of the coulombic efficiency (μ_i) is not constant but depends on the battery state (SoC, temperature, etc.). For lithium batteries, it is practically unity.
- The main problem with Coulomb Counting is that it does not account for any potential error in the current measurement. In particular, a sensor offset causes a constant measurement error; this error, when integrated in an open-loop over time, causes the integral value to diverge.

The method can be used provided that periodic calibration is performed when the battery is in a known state, such as full charge. It is not guaranteed that this condition will be met in all applications. In such cases, Coulomb Counting is not the most suitable algorithm for SoC estimation. We will see later that it will be used in a feedback system to correct errors on SoCinit and current measurement.

Discharge Test

This technique involves a controlled discharge at constant current followed by a subsequent recharge. It is considered the most reliable method for estimating the state of charge. However, its major drawback is that it is not suitable for real-time applications. This is because one must wait for the duration of a discharge, and also because during the test, the battery is disconnected from the load (requiring a constant current), thus interrupting the functionality of the system.

Open Circuit Voltage Method

In low-power applications, which operate with small load currents, it is possible to determine the state of charge of the battery based on the open circuit voltage (OCV). There is indeed a relationship between SoC and OCV. The state of charge is related to the number of ions, which in turn determine the cell voltage. This correspondence allows for the exact value of SoC to be derived from a measurement of the open circuit voltage. However, obtaining an accurate measurement of OCV requires waiting for several hours, corresponding to the relaxation time of the cell when it must be disconnected from the load. Additionally, the OCV(SoC) relationship is nonlinear and exhibits a nearly flat region (depending on the chemistry) where a small range of voltage corresponds to a relatively wide range of SoC; in LiFePO₄ cells, this behavior is quite pronounced. In the region where $\frac{dOCV}{dSoC} \simeq 0$, a small

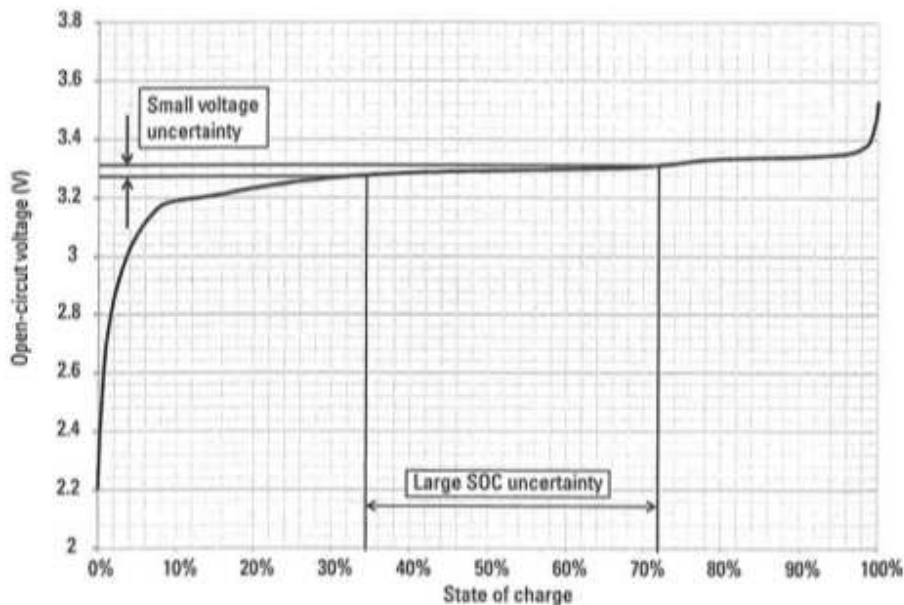


Figure 5.4: Open Circuit Voltage

change in voltage corresponds to a wide range of SoC, leading to a significant error in estimation. However, the simplicity of the method makes it advantageous in certain applications.

Model-Base

A model-based estimation method is useful when the application requires online estimation of SoC, meaning that the value of this parameter needs to be known during the normal operating phase of the system. The model must accurately reproduce the real behavior of the cell and, consequently, provide information (including state of charge) when it receives measurable battery quantities as inputs, namely voltage and current. The accuracy of the estimation depends on the accuracy of the model used, and various types of models can be found in the literature:

- **Electrochemical models:** These models describe the cell's behavior through equations that relate macroscopic parameters (voltage and current) to microscopic parameters related to the chemical-physical reactions within the cell, such as the number of electrons exchanged during redox reactions. While accurate, these models are extremely mathematically and computationally intensive, making them impractical for many applications.
- **Mathematical models:** In these models, the measured voltage and current are used to determine coefficients of mathematical and statistical functions that have little connection to the physics of the battery. They are used in very specific applications.
- **Circuit models:** The cell is represented by an equivalent circuit with lumped parameters. This allows for a correspondence with the physics of the device and, importantly, provides electronic designers with greater ease of understanding and implementation. Several equivalent battery circuit models can be found in the literature, but most have common elements: a controlled voltage source to represent the OCV, a series resistance, and one or more RC groups to model transient battery phenomena.

In this thesis work, a model with a single RC group was adopted. The left part of the circuit schematizes the charge in the cell as stored in the capacitor $C_n = \frac{Q_n}{1V}$. On the right part, the voltage generator V_{OCV} is controlled by the value of SoC and therefore represents the relationship between OCV and state of charge. R_0 is the series resistance and the RC group models the relaxation effects of the cell. The output voltage from the model is, therefore:

$$v_M = V_{OC}(SoC, T) - V_{R_0}(SoC, T, i_L) - \sum_i v_{RC_i}(SoC, T, i_L)$$

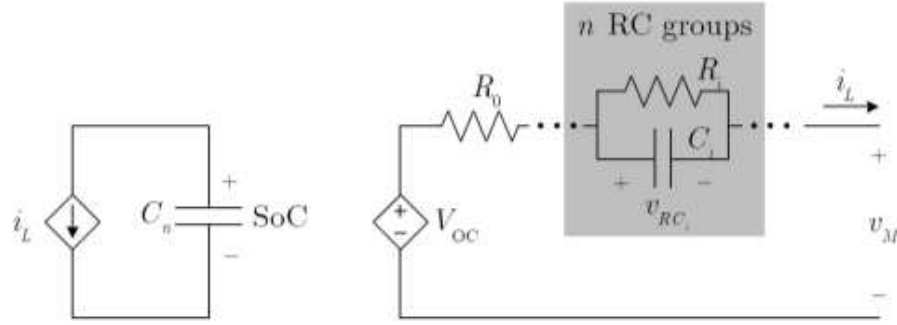


Figure 5.5: Model Base

The use of this estimation algorithm, with this circuit model, assumes that the output voltage from the model is equal to the cell voltage v_T . Therefore, by measuring v_T and the load current i_L , one can determine the value of SoC without resorting to the direct measurement of OCV, which, as mentioned, would require long waiting times.

Kalman's Filter

This method is used in many applications (monitoring, global communication, positioning, navigation, control systems) as it allows estimating the state of a dynamic system. This occurs recursively: a series of noisy data is processed through inequalities to provide a statistical estimation of the system's state. The inequalities are in the discrete-time domain and are solved recursively and in real-time. In the case of the battery, the estimated state variables could be SoC and SoH. At each sampling instant, the filter acquires the inputs and uses them along with those from the previous instant to calculate the output values. These outputs are compared with the measured values to derive the error, which is then used to approximate the system's state. The Kalman Filter (KF) is particularly suitable for linear systems. In cases where a system is not linear, it is necessary to apply a linearization process for each time instant, approximating the system as a Linear Time-Varying (LTV) system. The LTV system is then used in the KF. The entire process constitutes the Extended Kalman Filter (EKF), which is used in various state estimation algorithms for lithium-ion batteries.

Neural Network

The term "neural network" refers to a network of artificial neurons that can be implemented in software or dedicated hardware. These networks are capable of processing a large amount of data, and this computational power arises from their

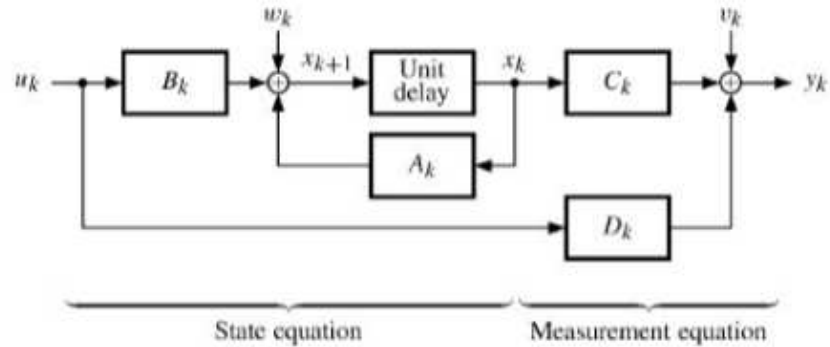


Figure 5.6: Kalman Filter

ability to work in parallel. Neural networks constitute a complex statistical system that is highly robust to noise and disturbances. The nodes are organized into hierarchical layers: there is an initial layer of neurons that receives the inputs, and this layer communicates with the next layer through interconnections, and so on. Each input is multiplied by a weight coefficient based on its importance. Using

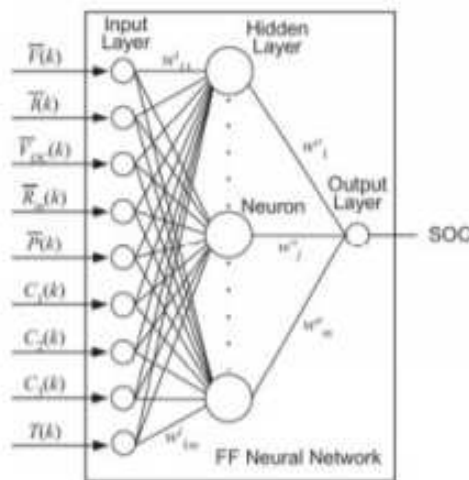


Figure 5.7: Neural Network

a neural network for estimating the state of charge of a battery can undoubtedly lead to very accurate results. However, due to the large number of nodes and connections involved (which can even reach thousands), implementation becomes very complex and costly.

Mixed Algorithm

A hybrid approach consists of using two methods, appropriately combined, to leverage their respective advantages. In electric vehicles, for example, estimating the SoC using Coulomb Counting can be effective in capturing rapid changes in the state of charge. In this application, the continuous alternation of accelerations and braking results in a jagged load current profile, so current integration allows for good tracking of this trend. However, Coulomb Counting suffers from the already mentioned issues related to initial SoC and current measurement error. In this thesis work, the correction on current integration is performed using a cell model, thus combining Coulomb Counting and model-based approaches, as proposed in [reference]; this algorithm will be further discussed in a subsequent chapter.

5.3.3 State of Health (SoH)

The state of health (SoH) is a parameter that provides information about the battery's life. The aging of the cell results in a progressive loss of capacity, meaning that, with usage and the passage of time, the maximum stored charge will decrease. Therefore, a good definition of SoH (State of Health) is based on the progressive loss of cell capacity.

$$SoH(t) \triangleq \frac{Q_{max}}{Q_n}$$

where $Q_{max}(t)$ is the extractable charge at time t and Q_n is the nominal capacity of the cell. Multiplying equation by 100 yields the SoH in percentage terms. Estimating SoH is very complex due to its dependence on multiple factors, foremost among them being the application for which the battery is used. Cell aging depends on the number of discharge cycles, the idle time during which the cell is in a self-discharge regime, the operating temperature, and the rest temperature. With aging, there is also an increase in the internal resistance of the cell; this phenomenon has led to techniques based on estimating this resistance and has allowed the definition of the state of health in an alternative manner.

$$SoH(t) = \frac{R_{EoL} - R(t)}{R_{EoL} - R_0}$$

where R_{EoL} is the end-of-life resistance of the battery, $R(t)$ is the estimated online resistance, and R_0 is the value of internal resistance when the cell is new. Methods for estimating the state of health can be based on an aging model; in this case, they can be broadly classified into two categories:

- An open-loop model that predicts the loss of capacity and the increase in internal resistance of the cell; the model can be chemical-physical, mathematical, or electrical.

- A feedback model similar to the mixed algorithm used for SoC estimation. A battery model is utilized along with advanced estimation techniques such as Kalman filters or least square method (LSM) techniques to calculate the model parameters in real-time.

Chapter 6

Analysis and Results of the Thesis Project

In the following pages, the practical work carried out on the product over these months is reported. The first phase involves characterizing the battery; then evaluating the SoC, accurately determining the amount of stored charge to have a general overview of the battery and verify if it is suitable for our purpose. In a second step, it is necessary to understand which circuit is best to connect the battery to the product and calculate the energy impact in terms of consumption, as it is an embedded device; and finally, it is necessary to characterize the Peltier cell and connect it to the application. Last but not least, understanding how to attach the device to the interior windshield glass, with the right angle to maximize the efficiency of the Peltier cell.

6.1 Battery characterization

Battery characterization was conducted using a battery with a nominal value of 1800mAh and 4 V. Two different systems were employed for this purpose:

- A system based on constant current discharge, performed using a dedicated test bench that will be analyzed later.
- A system based on constant resistance discharge.

6.1.1 Constant current discharge

The bench was built using an Arduino, which reads the battery voltage through an analog pin and controls a relay. The relay switches between the charging side, if the voltage is below 4.0V, and the discharging side, where it powers an active

load with a default fixed discharge current. The results of this hardware setup are displayed on an LCD screen. Additionally, the results are stored on an SD card.

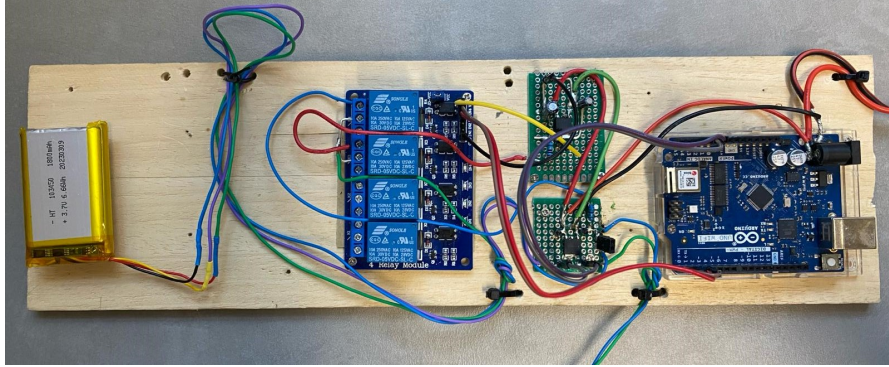


Figure 6.1: Hardware

The test was performed multiple times on the same battery and on different batteries with varying lifespans: new, used (2 months of use), and old (6 months of use). This was done to understand how the battery deteriorates over time. During charging, the battery is simply charged by the device’s built-in charger until it reaches the threshold of 4.15V. During discharge, the algorithm is slightly more complex. The charge Q is calculated according to the formula,

$$Q(t) = Q_0 - \int_0^T i_L(t)dt$$

and then the various charge samples for delta t are summed until the battery drops below the threshold of 2.7V.

Variable	Battery 1	Battery 2	Battery 3	Battery 4	Battery 5
Charge	usb	usb	usb	usb	usb
Discharge	Arduino	Arduino	Arduino	Arduino	Arduino
Time Discharge	02:25:20	04:40:46	04:30:30	04:35:45	05:04:02
V_{init}	4.08	4.152	4.158	4.163	4.14
V_{final}	2.7	2.67	2.65	2.68	2.78
Coulomb	3700	6568	6424	6548	7228
mAh Tot	1027	1824	1784	1812	2007

Table 6.1: Summary Application

6.1.2 The discharge with a constant resistance

The system is based on a setup where a set of resistors, connected in parallel, are linked to the battery along with a multimeter. The multimeter, set to sample data every 10 seconds, stores the collected data onto a USB drive. Once the battery is completely discharged, the data is processed using a MATLAB script developed by myself. This script meticulously analyzes all the data characterizing our battery using appropriate mathematical formulas. Furthermore, various plots are generated to better understand the battery's behavior. Within the MATLAB script, data related to the current flowing through the battery during the test, variations in voltage, the amount of charge the battery is able to accumulate, and the time delta required for the battery to fully discharge are processed. Of particular interest is the voltage-capacity characteristic, as illustrated in the graph.

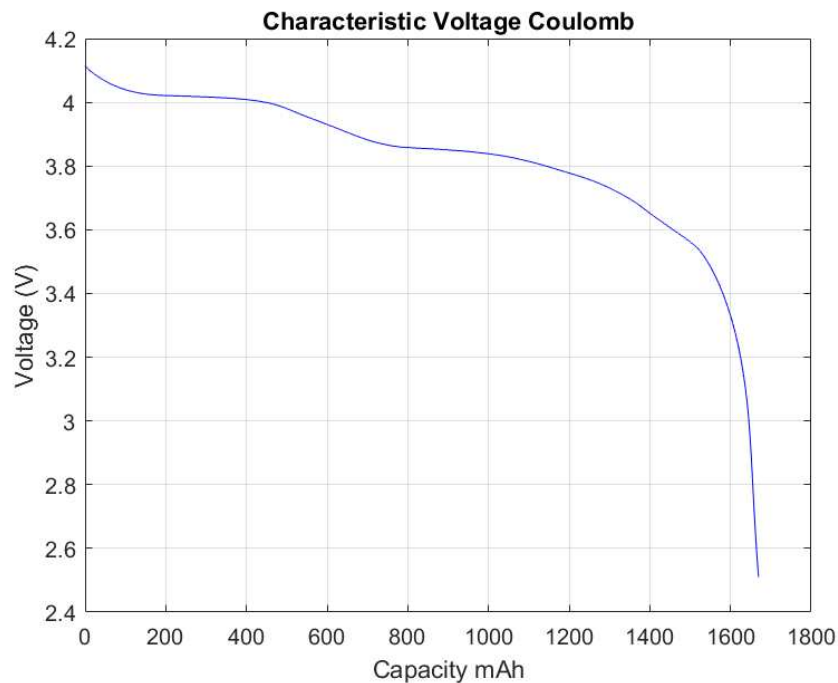


Figure 6.2: Discharge Curve

6.1.3 Consideration

As evidenced by the graphs depicted, the battery exhibits a trend similar to those on the market. It is worth noting that a fundamental parameter in the market is temperature, a factor that was not considered in this type of test as we are operating in a laboratory environment where the average ambient temperature is

approximately 22°C .

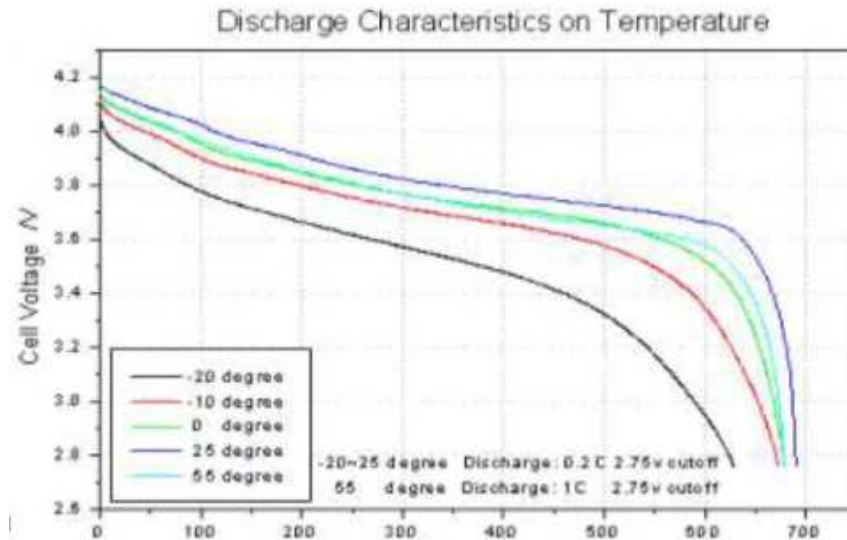


Figure 6.3: Discharge Curve General Market

A significant temperature test on our batteries is addressed in the following section. We notice that the curve exhibits significant bends that cause the battery voltage to drop from one value to a lower one, resembling small "kinks" in the middle of the curve. This poses issues in the application of our devices. Additionally, the kink occurs at an average voltage of about 3.4V, consistent with batteries available on the market. Despite being a battery with a nominal value of 1800mAh, we observe that the actual charge capacity it can store is approximately 1670mAh. This value is unsatisfactory for us as our objective is to have a long-lasting battery powered by environmentally friendly elements such as Peltier cells or solar panels. In the previously discussed point, the thesis that the charge capacity is lower than the nominal one is further confirmed by test 2), where applying a fixed current of 400mA resulted in the battery discharging in about 4 hours with a total charge capacity of approximately 1700mAh, aligning with the earlier observations. We have chosen to explore other suppliers and analyze different batteries. Below, I only present the plot of the charge capacity, a fundamental parameter for us.

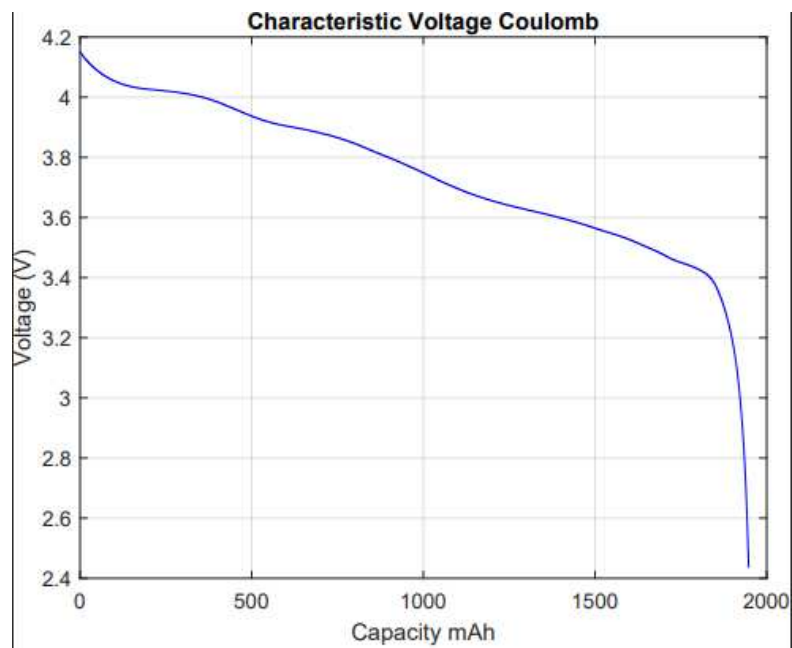


Figure 6.4: Discharge Curve

Below is the graph comparing the two batteries.

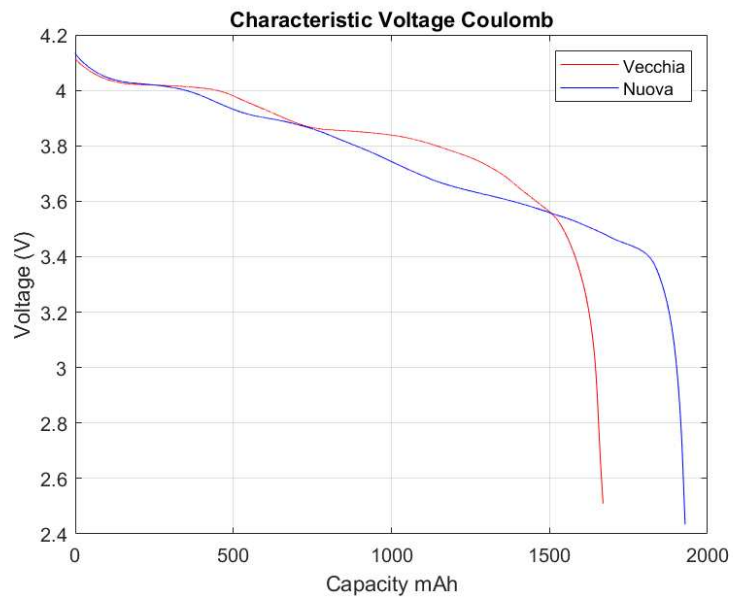


Figure 6.5: Comparison

6.2 Battery Temperature Test

Following the characterization described above, another aspect to consider is the temperature. It is necessary to test the actual thermal resistance of the battery because the device must be placed inside a car cabin, attached to the windshield, and in the worst-case scenario, it could be summer and already outside the cabin at 40°C , so inside almost 60°C . In that case, what temperature will the device reach? And will the battery be able to handle these high temperatures or will it be a further reason for deterioration? To analyze these issues, I have set up a bench where, through a state machine implemented on Arduino, relays are controlled to charge or discharge the battery following a specific charging cycle.

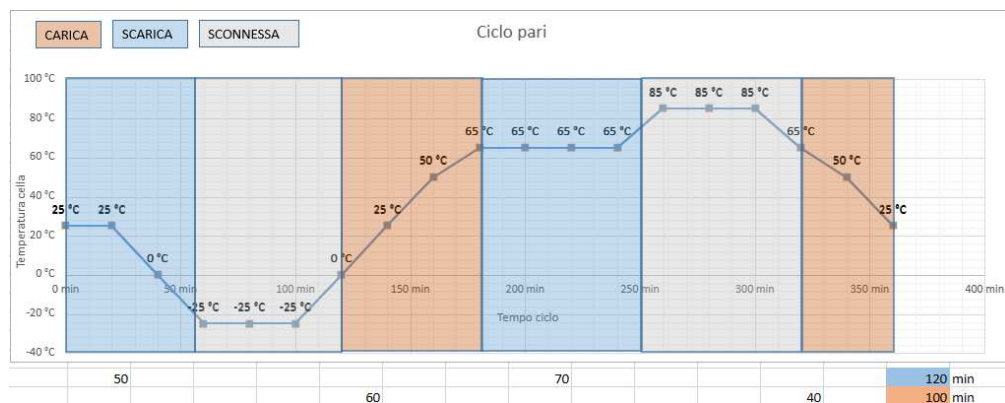


Figure 6.6: Test Curve

The batteries, along with an NTC sensor, are placed inside an oven programmed to perform discharge and charge cycles as shown in the graphs.

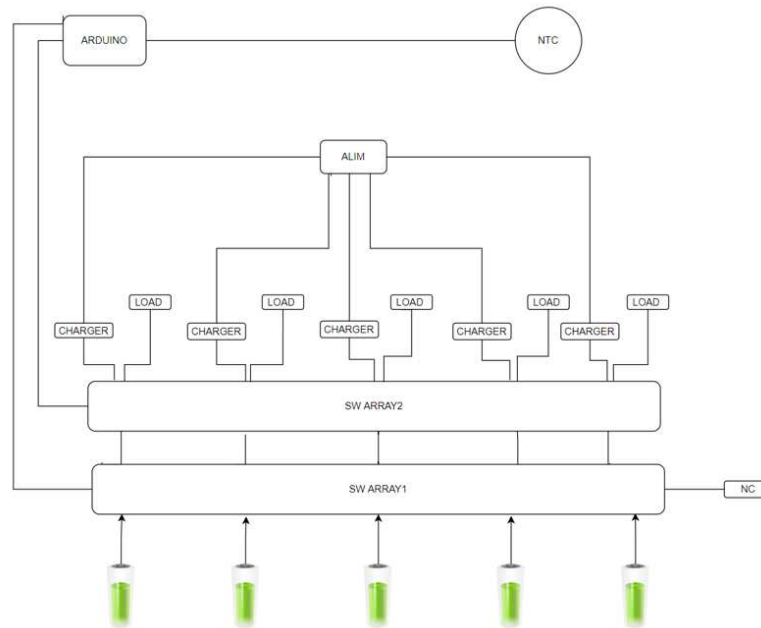


Figure 6.7: Block Diagram

This is the initial draft of the schematic where we test 5 batteries connected to relays that activate the charging channel or battery discharge based on the command sent by Arduino. The Arduino software is controlled by the external temperature read by the NTC, according to the graphs reported above. In detail, we can see that each individual relay is connected as follows.

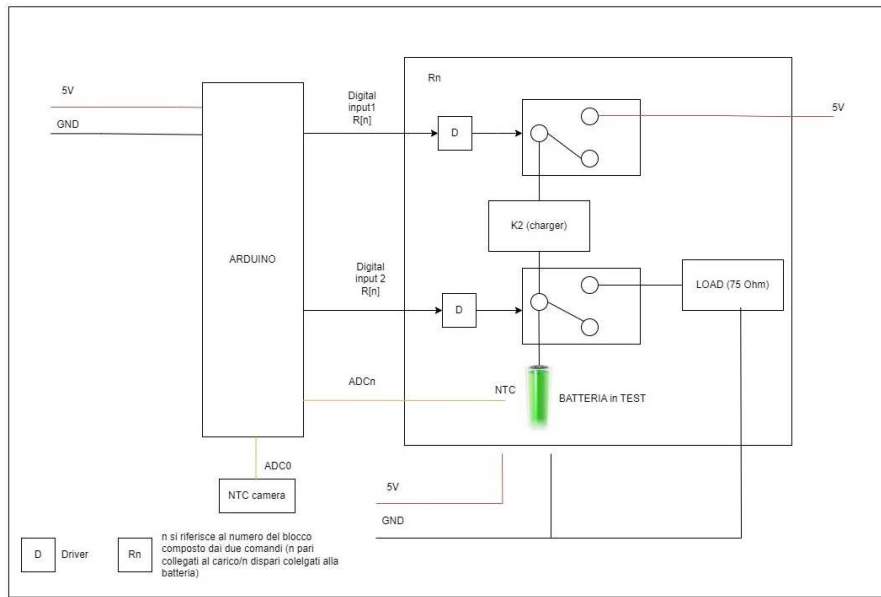


Figure 6.8: Switch Block Diagram

Below is the test bench I created where the test runs were performed to ensure everything worked correctly. Once the system was validated, my colleagues set up the more complex system described above with 5 batteries in the laboratory.

6.2.1 Result

The results obtained are promising; the batteries inside the oven, exposed to high temperatures in continuous cycles, did not show signs of deterioration or swelling. This result is crucial for the continuation of this study because it allows us to better analyze the Peltier cells at elevated temperatures and begin to assess whether it is beneficial to place the cell on the windshield on the cold side or the hot side.

6.3 Characterization Peltier Cell

In contrast to Chapter 3, here we present formulas applied to the Peltier cell that allow us to analyze our specific use case. When purchasing a Peltier cell, it is important to consider four fundamental factors that determine its efficiency:

1. Q_{max} : This is the maximum heat transfer capacity (expressed in Watts) from the cold side to the hot side.
2. V_{max} : This is the most efficient voltage (expressed in Volts).

3. I_{max} : This is the most efficient current (expressed in Amperes).
4. δT_{max} : This is the maximum temperature difference between the cold side and the hot side of the cell (expressed in Watts).

6.3.1 Example calculation of Peltier cells using simplified formulas

If we have an ambient temperature of $30^{\circ}C$, a power of $70W$, the heat from the CPU (cpuW) expressed in watts, and a thermal resistance of the heatsink at $0.7^{\circ}C/W$, we will have: The total heat dissipation from the heatsink is given by $T_{oth} = P + \text{cpuW} = 113 W$. The temperature at the hot side (T_1) is calculated as $T_1 = T_a + (C/W) \times (P + \text{cpuW}) = 109.1^{\circ}C$. The high value of T_1 ($109.1^{\circ}C$) indicates that the heatsink is not adequately dissipating the heat. To find T_2 (temperature at the cold side), we need to calculate the actual temperature difference ΔT_{real} , given by $\Delta T_{real} = (1 - \frac{\text{cpuW}}{P}) \times \Delta T_{max}$. Given $\Delta T_{max} = 65^{\circ}C$, the actual temperature difference is $\Delta T_{real} = (1 - \frac{43}{70}) \times 65 = 25.07^{\circ}C$. This indicates that there will be a 25-degree difference between the two faces of the cell, so $T_2 = T_1 - \Delta T_{real} = 84^{\circ}C$. At this temperature, the CPU would overheat. The value of T_{diss} (heatsink temperature) is calculated as $T_{diss} = T_a + (C/W) \times T_{oth} = 65^{\circ}C$. Since the temperature is still too high, to lower it, we need to choose a heatsink with a lower C/W or use a more powerful fan⁵

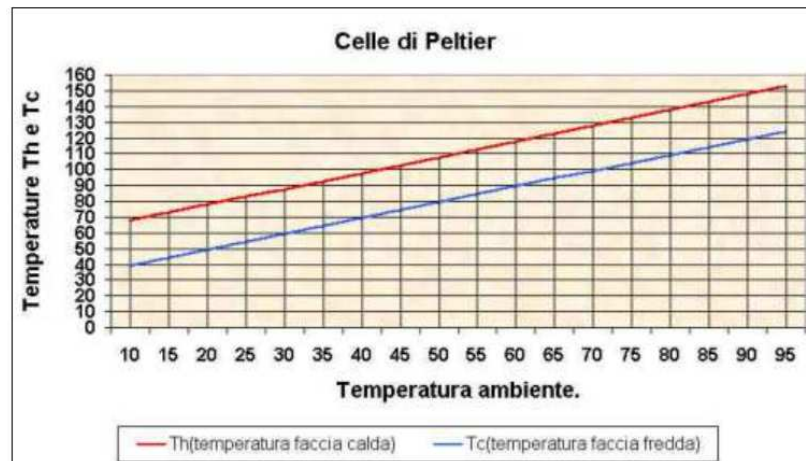


Figure 6.9: T peltier / T environment

⁵<https://www.megaoverclock.it/CELLEQUATTROUNO.html>

By varying the ambient temperature, we were able to examine how T_h and T_c vary. The thermal resistance of the heatsink and CPU wattage were considered constant.

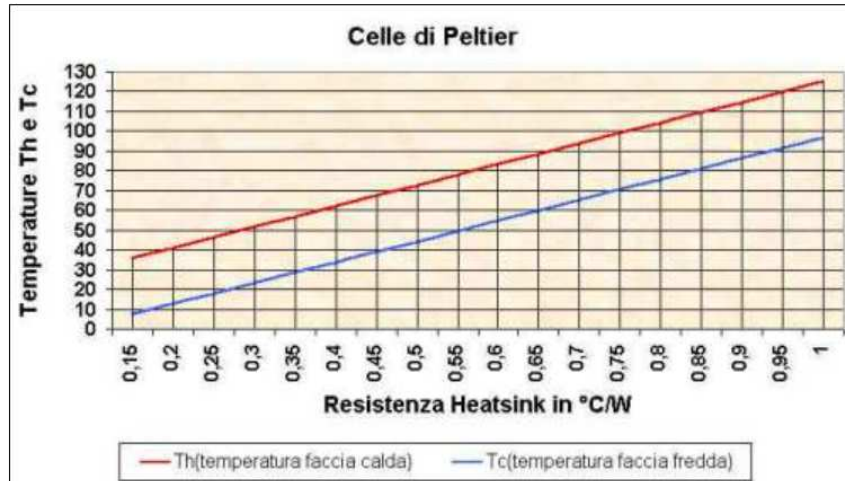


Figure 6.10: T peltier / Res Heatsink

By varying the thermal resistance of the heatsink, we obtained the following results. The ambient temperature and the heat produced by the CPU (CPU watts or Q_c) were considered constant values.⁶

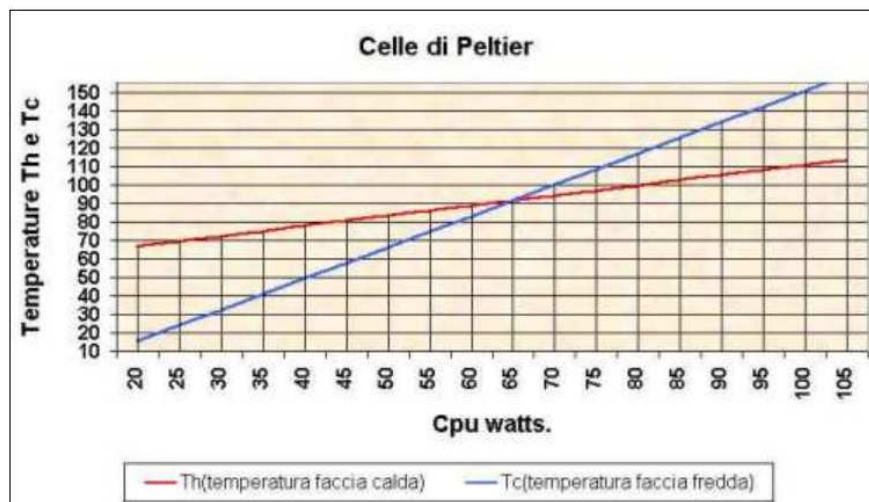


Figure 6.11: T peltier / CPU Watts

⁶<https://www.megaoverclock.it/CELLEQUATTROUNO.html>

By varying the CPU watts (Q_c), we can observe the change in T_h and T_c . The ambient temperature and the thermal resistance of the heatsink were considered constant values.

6.3.2 LT-Spice characterization

Unfortunately, the temperature characteristics of the Seebeck coefficient $\alpha_{Bi_2Te_3}$ and the electrical resistance of the thermoelectric couples $R_{Bi_2Te_3}$ are not provided to users by manufacturers as a general rule. Therefore, before they can be utilized in constructing an electrothermal model, they must first be determined through experimental characterization processes. To determine the temperature dependencies of the Seebeck coefficient $\alpha_{Bi_2Te_3}$ and the electrical resistance of the thermoelectric couples $R_{Bi_2Te_3}$, the test thermoelectric module (TEM) must be placed between two controlled objects over a wide range of temperatures T_c and T_h . From the measured output voltage V_o and electric current I , these two parameters can be derived as in the following formulas.

$$\alpha_{BiTe} = \frac{V_o}{(T_h - T_c)}$$

$$R_{BiTe} = \frac{V_o(I = 0) - V_o}{I}$$

Experimental measurement of the thermal conductivity $K_{Bi_2Te_3}$ poses many more challenges because its determination requires knowledge of a heat flow Q .

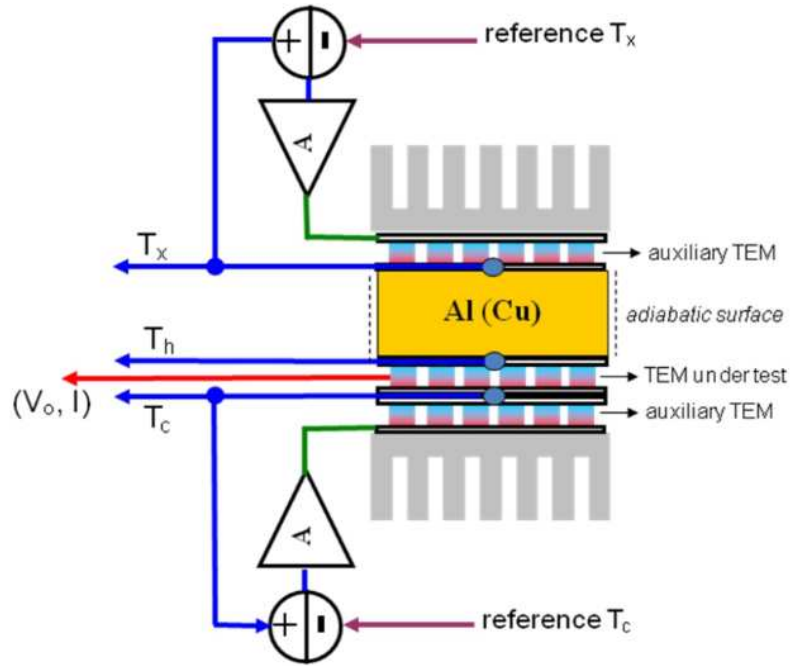


Figure 6.12: LT-Spice config

The temperature of the cold side of the thermoelectric module under test is controlled in a closed feedback circuit by an auxiliary thermoelectric cooler. The other side of the module is attached to an auxiliary thermal conductor block made of aluminum or copper, with surfaces. The other end of the block is attached to an auxiliary TEM with temperature T_x , which is higher than T_c . Given the thermal conductivity coefficient of the auxiliary conductor block, the heat flow can be easily obtained as in formula $Q_h = Q_x = \lambda_{Al}(T_h - T_c)$, which, upon substitution, yields in follow formula.

$$K_{B_i T_e} = \frac{\alpha_{B_i T_e} T_h I - \alpha_{Al}(T_h - T_c)}{(T_h - T_c)}$$

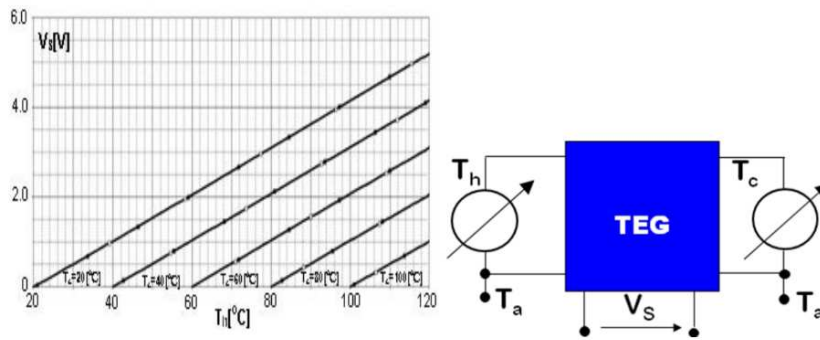
The temperature characteristics obtained for the three main parameters are approximated by second-order polynomial functions. The crucial part in the entire TEG design process is the modeling and electrothermal simulations capable of providing good estimates of the electrical energy obtained from heat conversion. A correctly designed generator requires many simulations during the design phase under various conditions to extract as much electrical energy as possible from a relatively low-efficiency system. In some cases, it can replace the prototyping of complex designs. In the following examples, some results of simulation experiments performed via electrothermal simulation are provided. They provide quantitative information on the behavior of the real TEG under different thermal and electrical

conditions, which often occur in practice. The polynomial functions appear in follow formula.

$$\alpha_{B_i T_e}(T) = -7 * 10^{(-7)} * T^2 + 1 * 10^{-4} * T + 49.1 * 10^{-3}$$

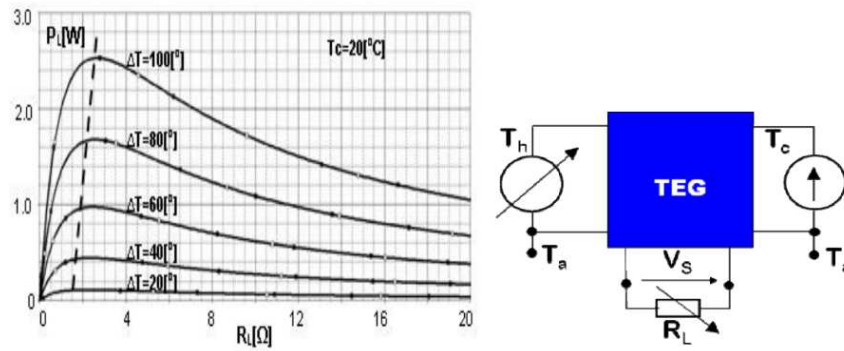
$$K_{B_i T_e}(T) = 4 * 10^{(-5)} * T^2 - 2.2 * 10^{(-3)} * T + 0.4626$$

"The output voltage V_S from the TEG for $R_L = \infty$ is shown in Figure. The simulations were performed for different temperature gradients by setting T_c as a parameter and T_h as discussed. Below is a schematic of the equivalent circuit for the simulations presented along with their characteristics".⁷

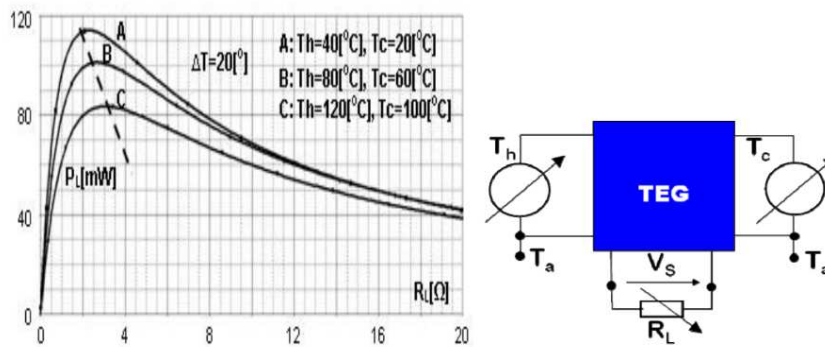


The graphs allow for estimating the maximum nominal voltage values when no resistive load is present. They can be very useful in the design of DC-DC boost regulators that step up the voltage to the level required by an electronic circuit, such as sensor nodes, for example. In Figure, output power P_L in relation to a resistive load R_L and different temperatures are depicted by gradients ΔT . From the simulated functions, the points of best match between R_L and the internal resistance of the Peltier module can be identified. It is worth noting that the point of maximum power transfer (MPTP) is not constant but moves towards higher R_L as the temperature gradient ΔT increases.

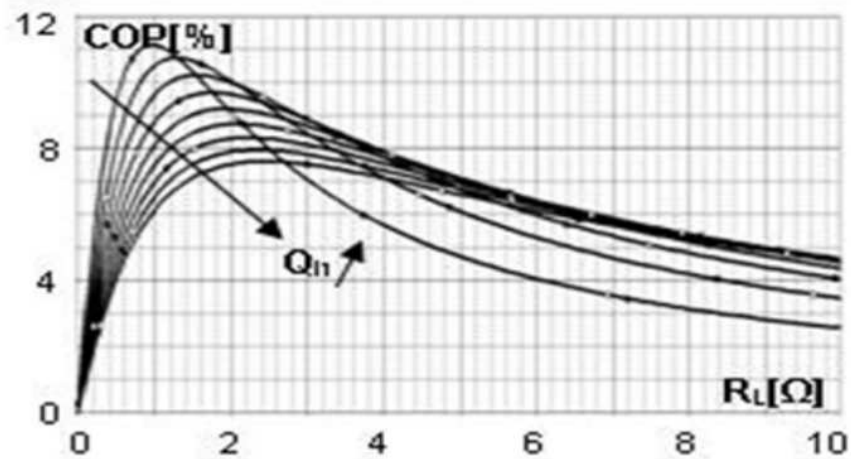
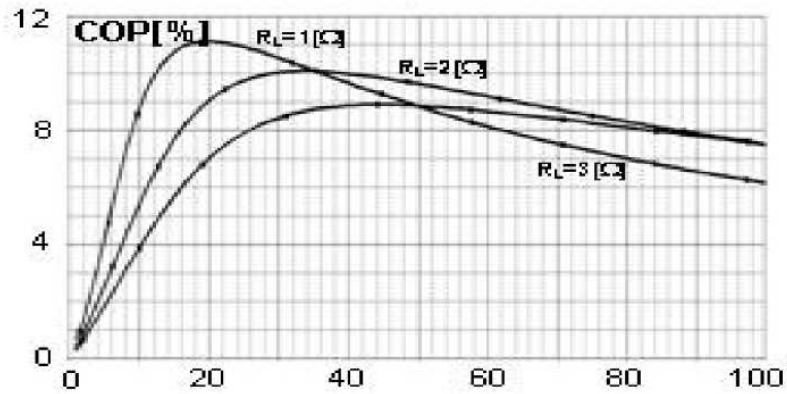
⁷Modeling and Simulation of Thermoelectric Energy Harvesting Processes



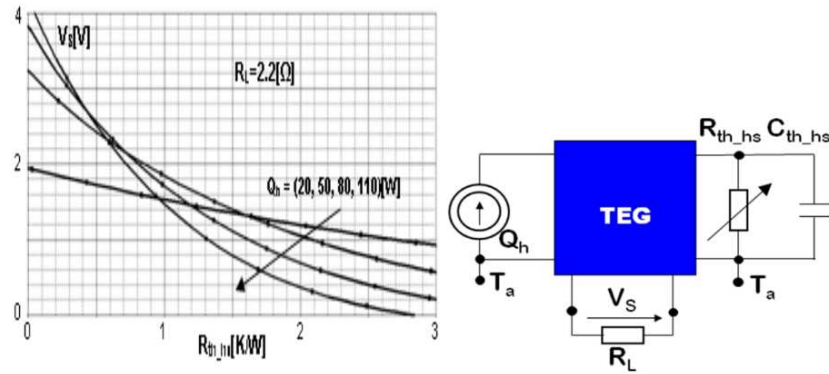
"Follow figure shows the output power P_L as a function of R_L for the same $\Delta T = 20^\circ$, at low, medium, and high temperatures. From this image, it is evident to designers that the maximum power delivered P_L depends not only on R_L and ΔT but also on the temperature range in which the temperature gradient ΔT is located."



The functions of the coefficient of performance (COP), defined as in. Both depict conversion efficiency in relation to a resistive load R_L and a heat power Q_h . It can be observed that the COP does not exceed 12



The results presented in Figure illustrate the importance of proper selection of the heat sink connected to the cold side of the module on the overall performance of the TEG. From the standpoint of output voltage, it appears that the thermal resistance R_{th_hs} of the heat sink should be chosen as low as possible so that the high thermal power Q_h translates into a sufficiently large temperature gradient across the Peltier module. Otherwise, a too high R_{th_hs} could waste the entire effort made to improve the overall efficiency of the system. On the other hand, it can be demonstrated that, similarly to the concept of electrical matching, the maximum power transfer can be provided if the thermal resistance of the heat sink is matched to the thermal resistance of the thermoelectric module.



6.3.3 The device structure with a Peltier cell

In this chapter, we begin to understand how the Peltier cell can interact with the ecosystem of the device by analyzing its power consumption, circuits, and all the fundamental aspects that allow us to extend the life of the battery with the goal of making the device self-sufficient. To ensure that everything works optimally, we need a driver that enables communication between the main microprocessor of the device and the Peltier cell. This driver exists and is specifically classified as one that enables energy harvesting. From Datasheet "This component is an ultra-low-power and high-efficiency energy harvester and battery charger, which implements the MPPT function and integrates the switching elements of a buck-boost converter. The device allows charging of any battery, including thin film batteries, by tightly monitoring the end-of-charge and the minimum battery voltage to avoid over-discharge and preserve battery life". Before applying the driver to the finished product, it is advisable to perform tests using its evaluation board. This allows us to determine if the component is indeed suitable for our purpose. Following the datasheet of the component and keeping in mind the considerations obtained regarding the Peltier cell, I modified the resistors of the evaluation board to extract the desired current values.

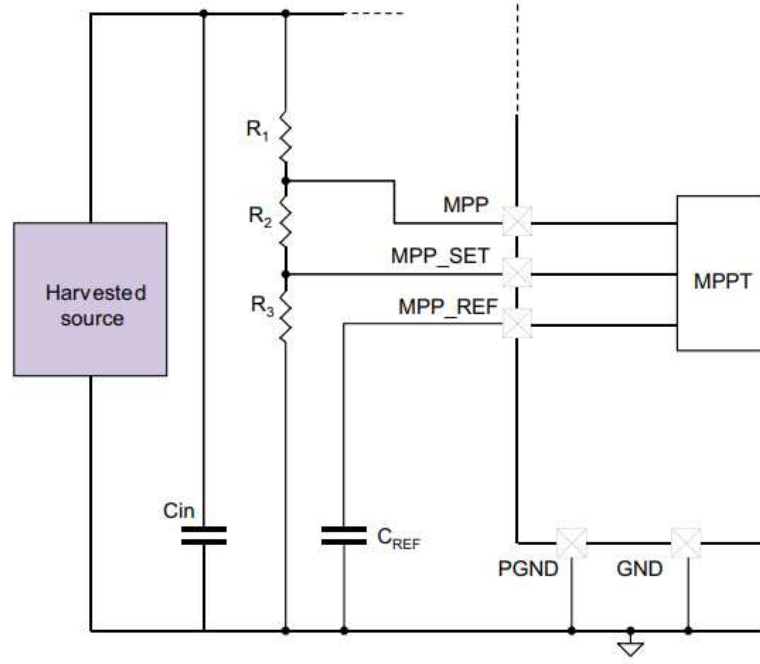


Figure 6.13: Harvesting Scheme

All this was done using the following formulas:

$$I_{Leak} = \frac{V_{oc}}{R_1 + R_2 + R_3}$$

$$R_3 + R_2 \leq (R_1 + R_2 + R_3) * \frac{V_{UVP(min)}}{V_{OC}}$$

$$R_3 + R_2 \leq 51 * (R_1 + R_2 + R_3) * \frac{V_{MPP(min)}}{V_{EOC}}$$

$$MPP_{Ratio} = \frac{R_2}{R_2 + R_3}$$

$$R_{eq} = \frac{V_{OC} - V_{MPP}}{I_{MPP}}$$

$$C_{in} = \frac{T_1}{R_e}$$

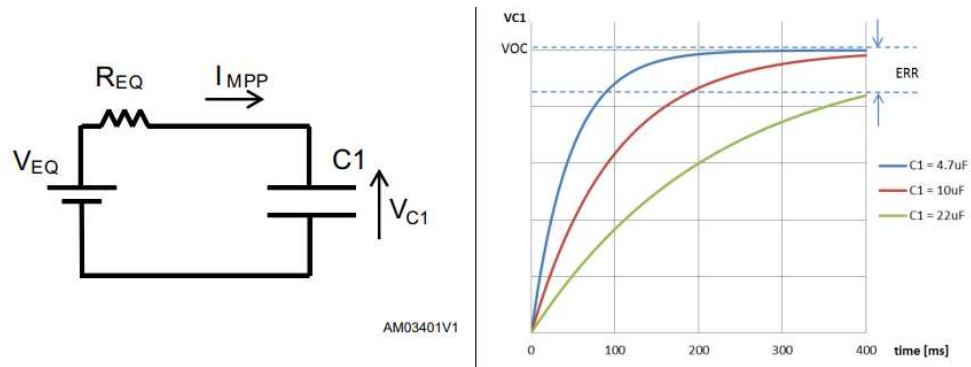


Figure 6.14: Harvesting Curve

6.3.4 Cell & Harvesting

Now, let's analyze how the Peltier cell behaves when driven by the chosen driver in the BOM of the product. In this case, we will analyze the same cell but under two different conditions. Firstly, we will analyze the Peltier cell with a heat sink placed on the hot side and a copper plate attached with thermal paste on the cold side. Secondly, we will maintain the heat sink on the hot side while applying a thermal pad on the cold side, also attached with thermal paste. The objective is to determine which of the two configurations allows the Peltier cell to deliver more current and which configuration is more suitable for our purpose, as the cell needs to be in contact with the windshield of the vehicle.

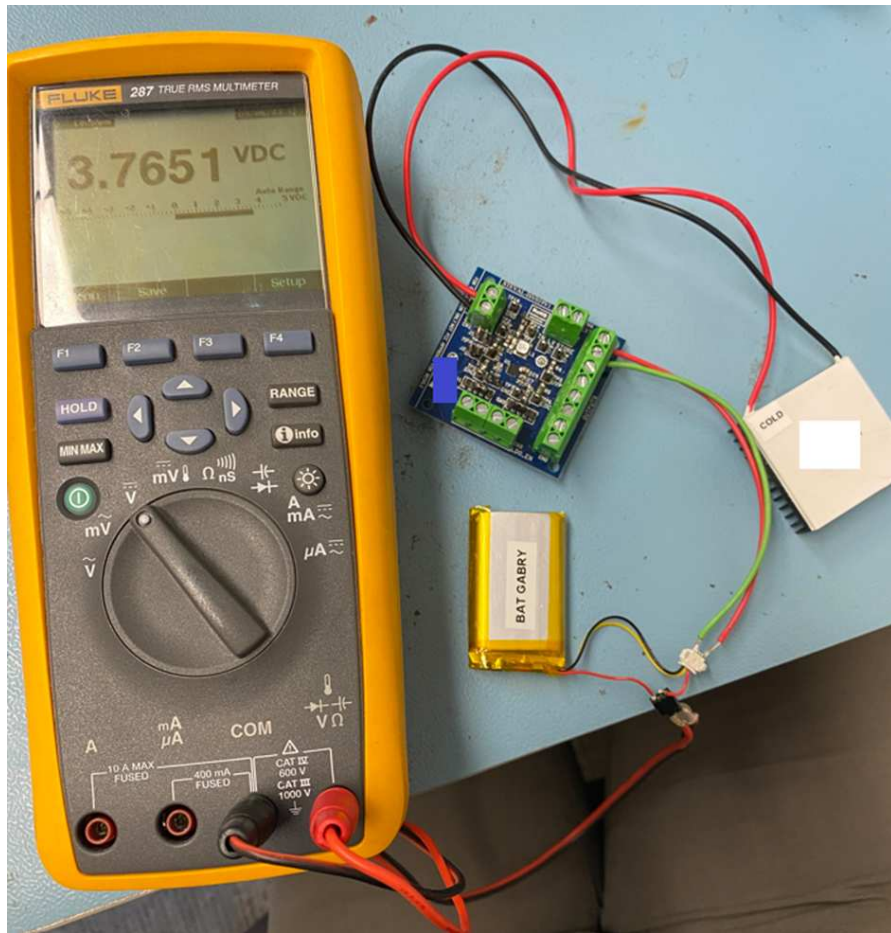


Figure 6.15: Test 1

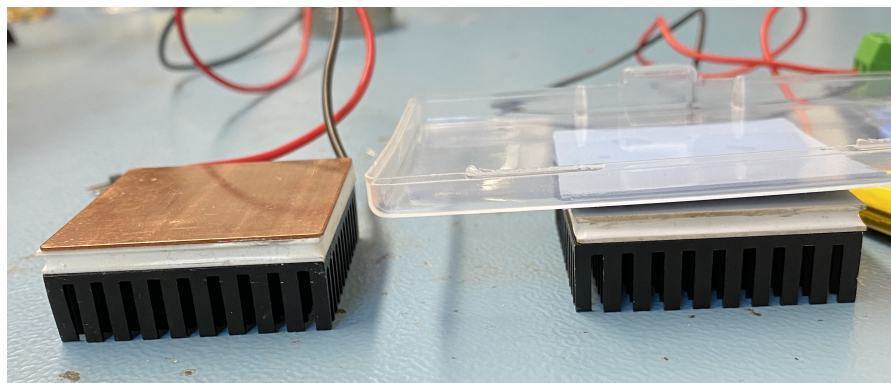


Figure 6.16: Test 2

The characterization of this circuit was conducted as follows: At the input of

the driver, there is the Peltier cell, which is heated using a hot air soldering station. Next, we have the driver with the set of changed resistors, while at the output, there is the battery (analyzed in the previous chapter) dissected and connected in parallel with a voltmeter. With this test setup, it is possible to determine how much voltage is being supplied to the battery by varying the temperature. Below is a table indicating all the parameters set during the test and their respective results. The following tests were performed by taking the circuit with the cell and the device shown in Figure, placing it in parallel with different resistors. Then, using a heat pump to blow hot air onto the Peltier cell, data were collected from the multimeter, which was also connected in parallel to the system (not the one shown in the photo).

Temperature	50°				Temperature	80°				Temperature	110°				
Delta	25				Delta	55				Delta	85				
Voltage	Current	Power	R (Ohm)	Voltage	Current	Power	R (Ohm)	Voltage	Current	Power	R (Ohm)	Voltage	Current	Power	R (Ohm)
48 mV	31 uA	1,49E-06	1	64 mV	59 uA	3,78E-06	1	100 mV	100 uA	0,00001	1	240 mV	47 mA	0,01128	4.7
64 mV	45 uA	4,1E-06	4.7	148 mV	25 mA	0,0037	4.7	240 mV	47 mA	0,01128	4.7	320 mV	60 mA	0,0192	10
94 mV	108 uA	1,02E-05	10	217 mV	36 mA	0,007812	10	320 mV	60 mA	0,0192	10	366 mV	72 mA	0,026352	22
100 mV	87 uA	8,7E-06	22	230 mV	42 mA	0,00966	22	366 mV	72 mA	0,026352	22	392 mV	85 mA	0,03332	56
108 mV	53 uA	1,17E-05	56	245 mV	44 mA	0,01078	56	392 mV	85 mA	0,03332	56	353 mV	63 mA	0,022239	68
66 mV	47 uA	3,1E-06	68	198 mV	34 mA	0,006732	68	353 mV	63 mA	0,022239	68	398 mV	67 mA	0,026666	100
93 mV	92 uA	8,56E-06	100	256 MV	47 mA	0,012032	100	398 mV	67 mA	0,026666	100				

Figure 6.17: Test 3

From the results obtained from the tests, as shown in the graphs and tables, it is possible to notice that the combination of the Peltier cell with the thermal pad performs better compared to the one with copper, and in our case, it is also more suitable for assembly, as we will see in more detail in the following paragraphs. However, the solution with copper is not to be discarded. In fact, copper in this context can act as a heatsink, which is useful in the system design.

6.3.5 Case

The device in question is an embedded system that needs to be mounted on the car windshield, so it must be a small device that does not obstruct the driver's visibility. Additionally, its thickness cannot exceed much for aesthetic reasons. Therefore, it is not possible to use the heatsink shown in the previous figures. The most effective solution is to place the cold side facing the windshield so that the glass heat can be absorbed by the cell and used to power the battery. The hot side should face the internal circuit so that when there is a high temperature difference between the two sides, the hot side can keep the temperature low in the internal circuit. Obviously, heat sinks need to be placed on both sides. On the hot side (internal side), a copper plate is used, while on the cold side (external side in contact with the windshield), a thermal pad is used. The mechanical structure of the device is

shown in the figure below:



Figure 6.18: Exploded View

In the exploded view, we can see the PCB of the device in green, which is hidden for corporate reasons. The yellow part represents the bottom part of the mechanical structure, made of plastic, and it has a central rectangular hole where the Peltier cell is placed. The cell is securely held from the internal side by a channel of about 2 mm, while on the external side, it is fixed using the thermal pad and thermal paste applied on both the face and the sides. To attach the entire device to the windshield, two adhesive tapes are added.

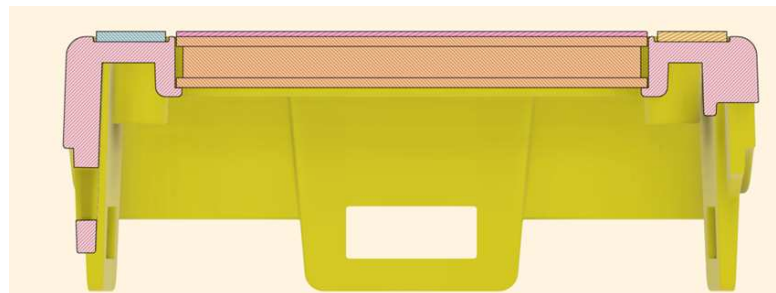


Figure 6.19: Transversions Section

In the cross-sectional view, we can better appreciate how the device comes into contact with the windshield and how the cell remains secure and wedged between the mechanical structure and the device.

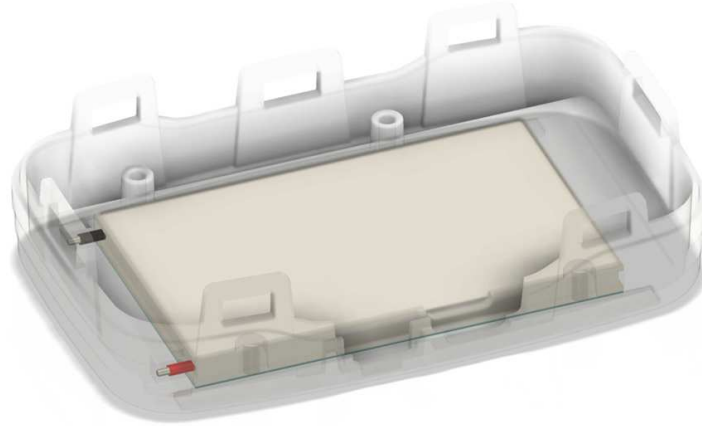


Figure 6.20: Scan View

Here we see how the Peltier cell is inserted into the mechanical structure, while in photo B, it is wedged in place through the channel we discussed earlier.



Figure 6.21: Case

Circuit

Below is the circuit fragment that allows us to see which components enable the cell to be connected to the entire device. For company reasons, I am unable to show in detail the names and values of the components. In the device, there is an ADC (Analog-to-Digital Converter) that reads the voltage value from the cell every 10 seconds and stores it in the internal memory until it is read via BLE terminal.

Conclusion

Unfortunately, despite having developed functional prototypes, the project outlined in this thesis will never come to fruition, at least not under these conditions. From a mechanical standpoint, the Peltier cell proves to be too bulky for the dimensions of our device. Although its dimensions occupy a larger area, the thickness of 4mm plus the 1mm thickness of the copper heat sink and thermal pad (the latter being negligible as its thickness aligns with that of the adhesive and presses optimally against the vehicle's windshield) is not feasible. From a technological and theoretical perspective, the idea appears to be promising. However, in practice, it falls short. As shown in Figure 6.17, the thermal delta required between the two faces of the cell must be very high to produce the energy needed to power the device's internal battery. Such temperatures are reached inside the vehicle during the summer but as total temperatures and not as a temperature delta. Additionally, external factors such as the vehicle's air conditioning during the summer months, which, when directed towards the windshield, causes a decreasing temperature difference between the faces, need to be considered. Similarly, in winter, the desired thermal difference cannot be achieved. Moreover, external factors such as the vehicle's air conditioning during the summer months, which, when directed towards the windshield, causes a decreasing temperature difference between the faces, need to be considered. Similarly, in winter, the desired thermal difference cannot be achieved. Continuing with mechanical considerations, we must also address the installation of the device on the vehicle's windshield. It must be positioned in a way that does not obstruct the driver's view, obviously not behind the front mirror, as in most modern cars, there is a black tint at that point, making the adhesion of the cell to the windshield less effective. The cell must adhere well to the windshield so that its entire surface is in contact with it to accumulate as much heat as possible. There is no need to apply thermal paste, glue, or anything else, as the device adheres perfectly to the windshield via the adhesive, leaving no thickness in contact with the cell. Regarding European regulations, we must consider that the device in question is a tolling system, which means it contains antennas that must comply with European standards. These parameters include antenna power, attenuation (all expressed in dB), and the device's inclination, all to ensure optimal antenna transmission. Unfortunately, this affects the study conducted in this thesis project because the Peltier cell, due to technological reasons, must be in contact with the windshield, thus covering the antennas and limiting their power and signal. Tests were conducted in appropriate venues, with anechoic chambers and all systems allowing for correct simulation, also yielding credible results for the project but not meeting the values required by European regulations. Therefore, as stated at the beginning of the chapter, the project will never come to fruition under these conditions, but new energy harvesting formulas are being actively considered to

address the problem.

Appendix A

Reference

1. "Introduction to vibration energy harvesting", Author: E. Blokhina, A. El Aroudi, E. Alarcon, D. Galayko, 2016
2. "Seebeck Effect", Wikipedia
3. "Modeling and Simulation of Thermoelectric Energy Harvesting Processes", Author: Piotr Dziurdzia, 2011
4. "Energy Harvesting con le celle di Peltier", Author: D. Scullino, 2016
5. "Solar Energy Harvester for Industrial Wireless Sensor Nodes", Author: R. Ibrahim, Tran Duc Chung, Sabo Miya Hassan, K. Bingi, Siti Khadijah binti Salahuddin, 2016
6. "ENERGY GENERATION FROM PELTIER MODULE BY UTILIZING HEAT", Author: D. Vadhel, S. Modhavadiya, J. Zala, 2017
7. "Realizzazione di algoritmo per la stima dello stato di carica di batterie al litio con identificazione online dei parametri", Author: G. Luca Amoroso, 2015
8. "<https://www.megaoverclock.it/CELLEQUATTROUNO.html>"